

 **HITACHI** 02 241 1574

HITACHI POWER MOS FET

APPLICATION NOTE

HITACHI SEMICONDUCTOR

Robert ree page 1

Mo2SK133-25T48
are instock

- all other devices are
available. *Ken Marks*

02-720133

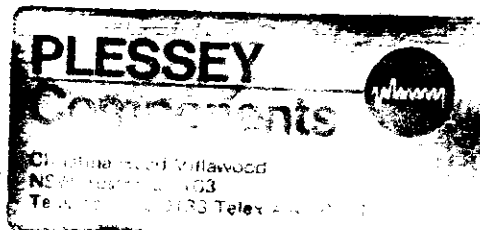


TABLE OF CONTENTS

1. Features of Power MOS FETs	1
2. Structure and Equivalent Circuit of Power MOS FET	2
3. Operational Features and Reliability	3
3.1 Output Characteristics	3
3.2 Frequency Response Characteristics	3
3.3 Switching Characteristics	4
3.4 Area of Safe Operation (A.S.O.)	4
3.5 Temperature Characteristics	4
3.6 Reliability	5
(1) Reliability design and process features	5
Chip structure	5
Chip fabrication process	5
(2) Reliability data	6
Failure criteria	6
Reliability test results	6
4. Application Hints	8
4.1 Design of High Power Application (Parallel Operation)	8
4.2 Design of High Breakdown Voltage Application (Series Operation)	8
(1) Totem pole connection	8
(2) How to reduce on-resistance in basic circuit	9
(3) Improvement of high frequency characteristics in totem pole connection	10
5. Reference Data	11
5.1 A.S.O. Limitation of Power MOS FETs	11
5.2 Thermal Mapping of Chip Surface Under Power Application	11
5.3 Input/Output Capacitance	12
6. Handling Precautions	13
6.1 Pin Arrangement	13
6.2 Measurement of Breakdown Voltage V_{DSX} and V_{GSS}	13
6.3 Observation of I_D - V_{DS} Characteristics	13
6.4 Circuit Experiments	13
6.5 Checking with Circuit Tester	14
7. Application of Power MOS FETs	15
8. Designing Application Circuits	16
8.1 Audio Power Amplifier	16
(1) Basic design philosophy	16
Frequency characteristics (frequency vs. gain, phase)	16
Consideration for parastic oscillation	16
(2) Typical design-1 (100W output at 100kHz, 0.01%)	17
Design of output stage	17
Design of voltage amplifier stage	18
Design of input stage circuit	18
Typical characteristics of experimental circuit	18
Precautions in fabrication	18
(3) Typical design-2 (50W output at 50kHz, 0.01%)	19
(4) Recommended line-up by output power	21
8.2 Power Oscillators (I)	22
(1) Basic design of power oscillation circuit	22
Oscillating conditions	22
DC bias conditions and AC amplitude	23
Determination of circuit parameters	24
Example of parameter calculation	24
Calculation of resonator capacitance	24

(2) Experimental circuit and typical characteristics (13.5 MHz, 40W)	25
8.3 Power Oscillators (II) (DC-DC Inverter)	25
Typical design	25
8.4 Medium-Wave Transmitters (Based on Data of NHK Technical Research Laboratories)	27
(1) Class D SEPP type pulse amplifier	27
Power amplifier circuit	28
Output variation by transformer winding ratio	29
8.5 High Power Switching Regulators Using Direct Rectification System	31
(1) Advantage of power MOS FETs	31
(2) Calculation of ideal characteristics	31
Typical values	32
(3) Typical design	32
Basic design philosophy	32
Cautions in fabrication	32
Circuit operation	32
Nominal characteristics of experimental circuit	38
8.6 Low-Noise DC-DC Converters	40
(1) Circuit configuration and operation	40
(2) Results of experiment	41

NOTICE

The example of an applied circuit or combination with other equipment shown herein indicates characteristics and performance of a semiconductor-applied product.

The Company shall assume no responsibility for any problem involving a patent caused when applying the descriptions in the example.

1 Features of Power MOS FETs

In developing power MOS FETs, Hitachi took note of the outstanding characteristics of small signal MOS FETs for high frequency amplification in TV tuners and FM tuners. After intensive research, we perfected high-output MOS FETs and introduced them as commercial products.

Hitachi's power MOS FETs have the line-up shown in Table 1-1. Each pair consists of an N channel type and a P-channel type, which have complementary characteristics.

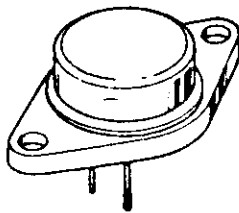
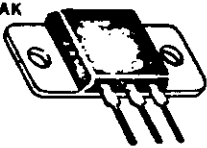
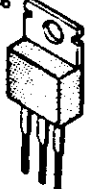
MOS FETs have the following advantages:

- Require a very low driving power as they are voltage-controlled devices.

- Free from current concentration, and hence have enormous resistance to destruction.
- Good frequency response and high switching speed due to absence of carrier storage effect.

These advantages make for the outstanding characteristics of power amplification devices. On the other hand, it is difficult to provide MOS FETs with the high voltage and high current characteristics required of power amplifiers. Hitachi succeeded in imparting these characteristics to MOS FETs by the method described in a later section of this application note.

Table 1-1 Series and Maximum Ratings of Power MOS FET

Type		Outline	I _D (A)	V _{DSX} (V) (V _{DSS} (V))	P _{ch} * (W)
N-Channel	P-Channel				
2SK133	2SJ48	JEDEC: TO-3 EIAJ: TC-3, TB-3 	7	120	100
2SK134/H	2SJ49/H		7	140	100
2SK135/H	2SJ50/H		7	160	100
2SK175/H	2SJ55/H		8	180	125
2SK176/H	2SJ56/H		8	200	125
2SK220/H	-		8	(160)	100
2SK221/H	-		8	(200)	100
2SK225	2SJ81	HPAK 	7	120	100
2SK226	2SJ82		7	140	100
2SK227	2SJ83		7	160	100
2SK213	2SJ76	JEDEC: TO-220AB EIAJ: SC-46 	0.5	140	30
2SK214	2SJ77		0.5	160	30
2SK215	2SJ78		0.5	180	30
2SK216	2SJ79		0.5	200	30

* Value at T_c=25°C

10-50
price

\$5-10

\$6.34

SK226 \$7-18
SJ56 \$

SK216 \$2.06
SJ79 \$2.06

50 off \$1.82 ea
Price

2. Structure and Equivalent Circuit of Power MOS FET

A problem encountered in commercializing a MOS FET for power applications is the required high-voltage and high-current characteristics.

The high-voltage characteristics will be explained with reference to the cross section of a power MOS FET in Fig. 2-1. The gate oxide layer (SiO_2) of an FET withstands a voltage of 20 ~ 30 V at best. As shown in Fig. 2-1, a power MOS FET has an offset-gate structure in which the drain and gate are separated. And between the separated gate and drain, a dopant is implanted by ion implantation, to create an ion-implanted layer so as to ease electric field concentration. Moreover, to prevent electric field concentration near the gate, a field plate is provided. In this way, destruction of the gate oxide layer is avoided and high voltage durability is achieved.

High current characteristics are obtained by a comb-structure of source-drain pattern. Fig. 2-2 shows the equivalent circuit of N channel device, r_g is the AC resistance of gate electrode, and C_{gs} is the equivalent capacitance of gate oxide layer.

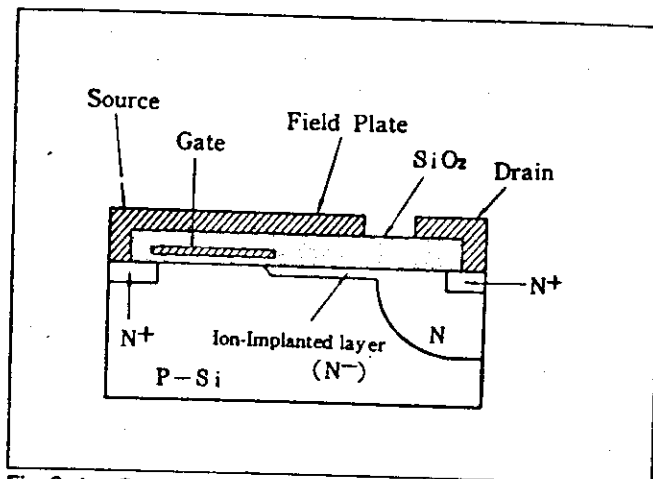


Fig.2-1 Cross section of a Power MOS FET
(Example of the N-Channel Device)

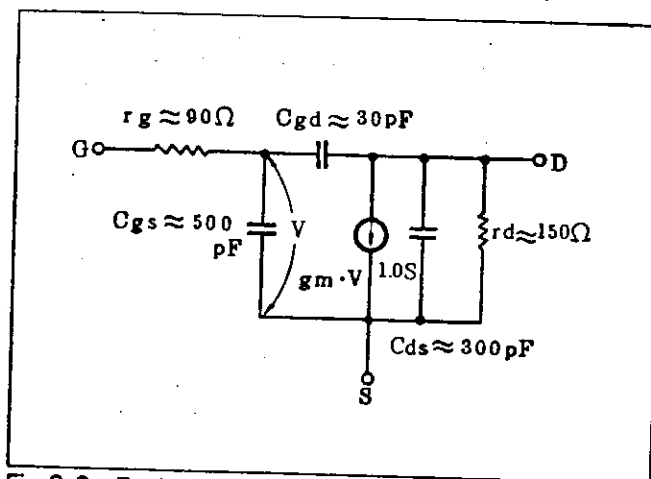


Fig.2-2 Equivalent Circuit of Power MOS FET
(Example of 2SK135)

3 Operational Features and Reliability

3.1 Output Characteristics

Figs. 3-1 and 3-2 show the output characteristics of the N-channel MOS FET 2SK135. Whereas in a small signal MOS FET the forward transconductance y_{fs} is 10 ~ 20 mS (milli-siemens) at best, in a power MOS FET it is 1.0 S. Also, as obvious from Figs. 3-1 and 3-2, 2SK135 has pentode characteristics and an excellent linearity of y_{fs} in relation to I_D .

P channel MOS FETs also have similar characteristics. P channel and N channel types have complementary characteristics.

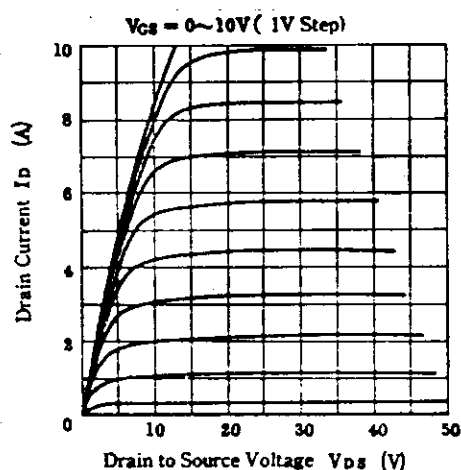


Fig.3-1 Typical Output Characteristics (1)

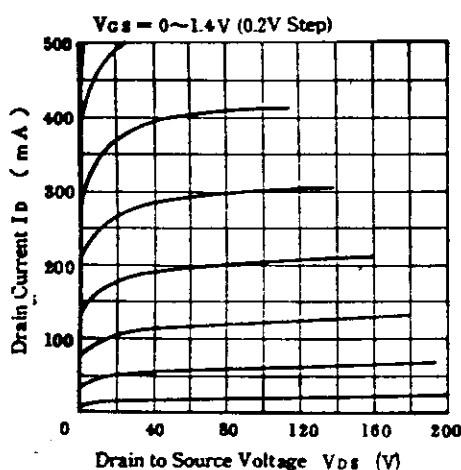


Fig.3-2 Typical Output Characteristics (2)

3.2 Frequency Response Characteristics

Fig. 3-3 shows the frequency response characteristics of a power MOS FET in the source common state. The cut-off frequency of an N channel device is about 3 MHz. The frequency response is dependent on the gate resistance and input capacitance shown in Fig. 2-2.

In the output stage of an audio amplifier, a source follower is used. The frequency response of the source follower is 10 times greater than in the case of source common because, as shown in Fig. 3-4, input capacitance is reduced by the mirror effect. The frequency response of a power MOS FET is more than one order better than that of a bipolar transistor.

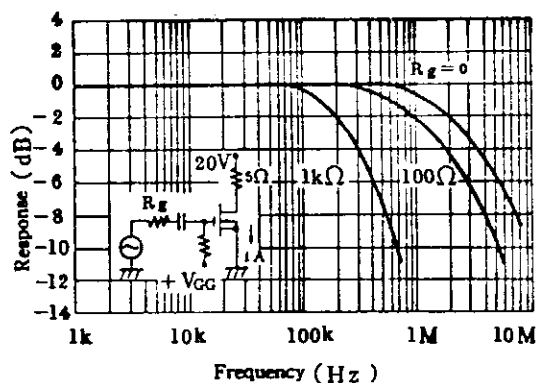


Fig.3-3 Frequency Response Characteristics of $1y_{fs}$ (Source Common)

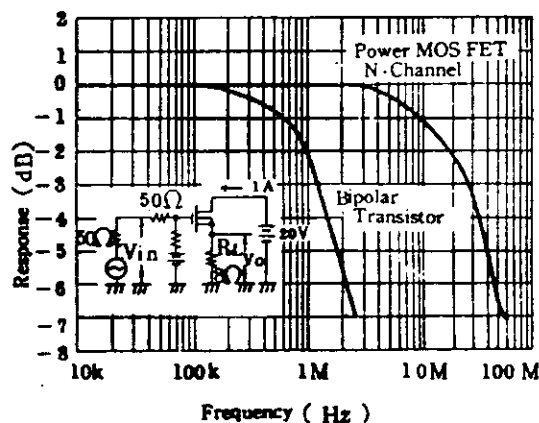


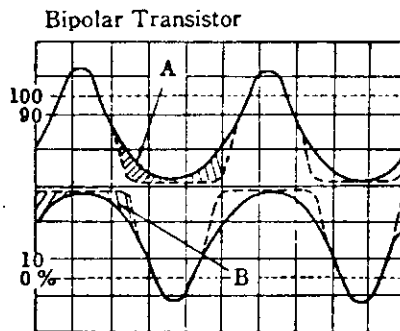
Fig.3-4. Frequency Response Characteristics of Source Follower

3. Operational Features and Reliability

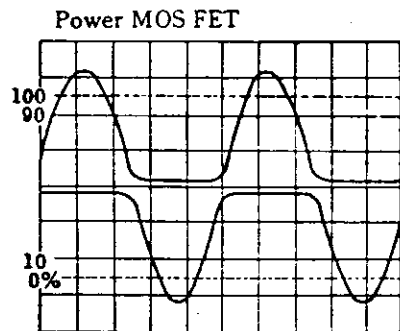
3.3 Switching Characteristics

A power MOS FET has no minority carrier storage and can switch a 2 A current at speed of 10 ~ 30 ns. This switching speed is 50 ~ 100 times as high as that of a bipolar transistor and represents a great advantage when a power MOS FET is applied to various high-speed large-power switching circuits, such as described later in this application note.

Fig. 3-5 shows current waveforms where a power MOS FET is applied to a class-B amplifier stage of an audio amplifier. The waveform is ideal for a power MOS FET which, unlike a bipolar transistor, has no storage time.



(a) Emitter Current Waveform



(b) Source Current Waveform

$f = 100 \text{ kHz}$ Vertical = 0.5 A/div
Horizontal = $2 \mu\text{s/div}$

Region A: Delay by Carrier Storage

Region B: Compensated by Negative Feedback

Fig. 3-5 Current Waveform of Class-B Amplifier Stage

3.4 Area of Safe Operation (A.S.O.)

Since a power amplifier device is operated at high voltage and high current levels, it must be designed to withstand electrical destruction. A power MOS FET basically takes full advantage of its excellent thermal stability, so that a much wider area of safe operation can be guaranteed for it than for a bipolar transistor.

Fig. 3-6 shows the areas of safe operation for DC operation and pulse operation. Since a power MOS FET is free of secondary breakdown in the high voltage region, the guaranteed area of safe operation is equal to the range of thermal limitation.

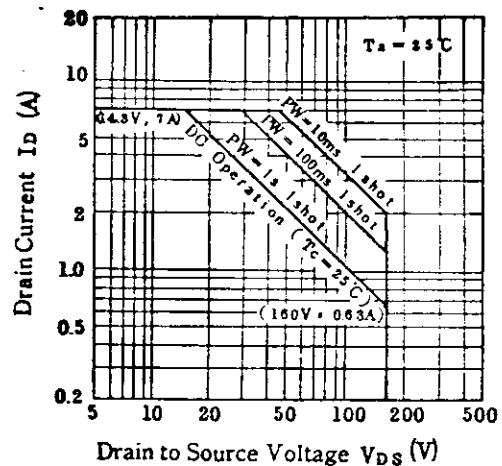


Fig. 3-6 Area of Safe Operation (2SK135/2SJ50)

3.5 Temperature Characteristics

Fig. 3-7 shows the transfer characteristics of power MOS FETs. In the high current area, the temperature coefficient is negative and current concentration does not occur, so that a wide area of safe operation is provided and destruction by thermal runaway is largely prevented. Since the transfer characteristics of power MOS FETs are of the enhancement type, as in the case of bipolar transistors, power MOS FETs do not require a complex biasing circuit as depletion type FETs do.

In power MOS FETs, the temperature coefficient of drain current becomes zero around $I_D = 100 \text{ mA}$.

By taking advantage of these temperature characteristics, the power MOS FET circuit can dispense with an idling current compensation circuit and feedback resistance for current stabilization, which are required in the bipolar transistor circuit as shown in Fig. 3-8. Hence, a simple circuitry as shown in Fig. 3-9 is obtained.

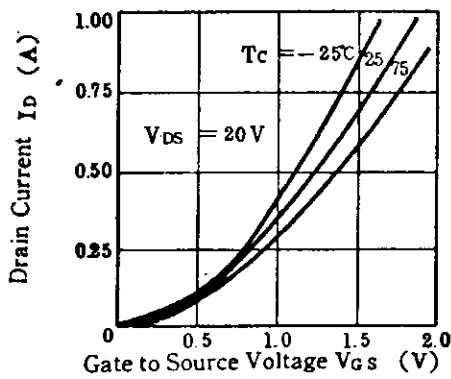


Fig.3-7 Typical Transfer Characteristics

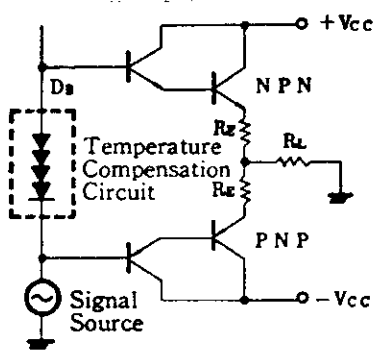


Fig.3-8 Audio Output Circuit using of Bipolar Transistor

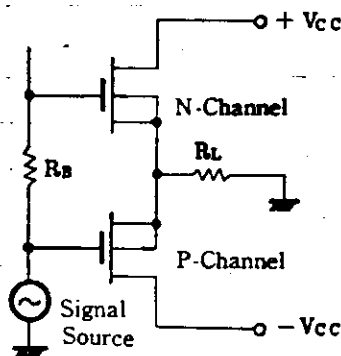


Fig.3-9 Audio Output Circuit using of Power MOS FET

3.6 Reliability

High quality and high reliability are achieved in power MOS FETs by applying the process technology and quality control established for MOS LSI and bipolar power transistors.

In order that you may use Hitachi's power MOS FETs with high reliability, explanation will be given by referring to reliability test data.

(1) Reliability design and process features

The chip structure of a power MOS FET is illustrated in Fig. 3-10. In order to achieve high voltage durability and high output characteristics, the following design and process considerations are given:

• Chip structure

To ease electric field concentration between source and drain, a low-concentration dopant is implanted by ion implantation, to form an offset gate structure. Further, by providing a source field plate, high voltage durability is achieved.

• Chip fabrication process

Since micropatterns and integration degrees similar to those of LSI are used, basic process technologies established for MOS LSI, such as surface passivation and electrode formation, are applied.

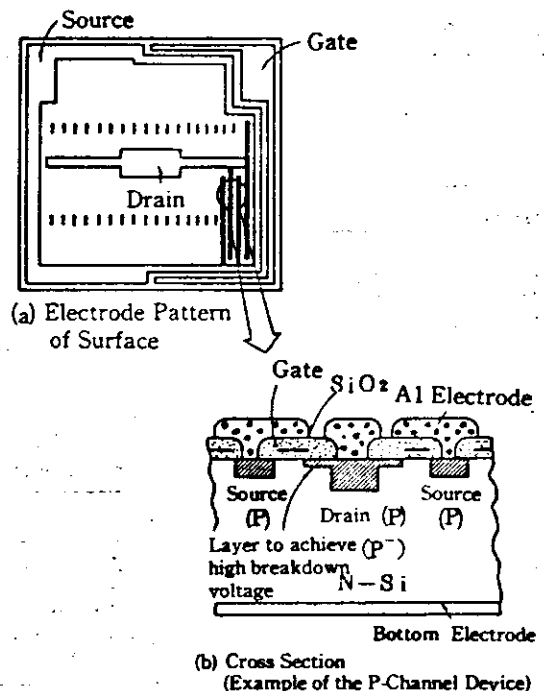


Fig.3-10 Pattern of Surface and Cross Section of Power MOS FET

3. Operational Features and Reliability

(2) Reliability data

• Failure criteria

Items for reliability tests and failure criteria are presented in Table 3-1.

Table 3-1 Failure Criteria

Item	Symbol	Failure Criteria (Note)		Unit
		Lower	Upper	
Breakdown Voltage	$V_{(BR)DSX}$ $\pm V_{(BR)GSS}$	$L \times 0.8$	—	V
Leak Current	I_{DSX} $\pm I_{GSS}$	—	$U \times 2$	μA
Cut-off Voltage	$V_{GS(off)}$	0	$U \times 1.2$	V
Saturation Voltage	$V_{DS(sat)}$	—	$U \times 1.2$	V
Saturation Voltage Ratio	$\Delta V_{DS(sat)}$	-30	+30	%
Forward Transfer Admittance	$ y_{fs} $	$L \times 0.8$	$U \times 1.2$	S
Forward Transfer Admittance Ratio	$\Delta y_{fs} $	-30	+30	%

(Note) U: Upper Limit After the Test
L: Lower Limit After the Test

• Reliability test results

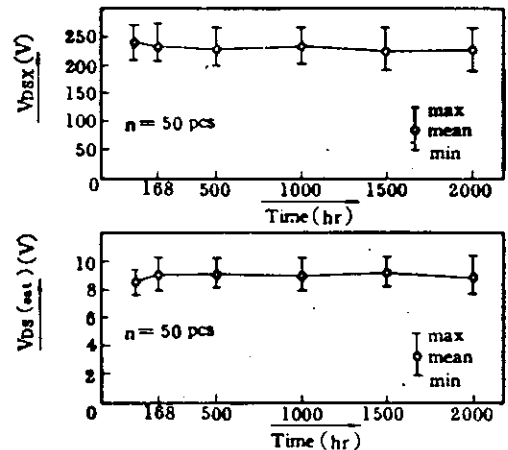
The results of reliability tests on complementary pair power MOS FETs 2SK135/2SJ50 are given in Table 3-2.

Table 3-3 shows the temporal changes of major parameters in device life tests.

Table 3-2 Test Results

Item	Test Conditions	N-Channel (2SK135)			P-Channel (2SJ50)		
		Sample Number (pcs)	Testing Time (hr)	Failure (pcs)	Sample Number (pcs)	Testing Time (hr)	Failure (pcs)
Operating Life Test	$T_a=25^\circ C$, $P_{ch}=27W$, $V_{DS}=80V$ Heat Sink $\theta_f=3^\circ C/W$ ($T_j=150^\circ C$)	80	2,000	0	100	2,000	0
High Temperature Reverse Bias Test	$T_a=150^\circ C$, $V_{DSX}=160V$, $V_{GS}=-10V$	125	2,000	0	140	2,000	0
Humidity Test	$T_a=80^\circ C$, $RH \geq 90\%$	77	2,000	0	77	2,000	0
Low Temperature Storage Test	$T_a=-55^\circ C$	45	2,000	0	45	2,000	0
Thermal Fatigue Test	$\Delta T_C=90^\circ C$, $T_{jmax}=150^\circ C$ ON: 1 minute, OFF: 1.5 minutes	50	10k cycles	0	50	10k cycles	0
Temperature Cycle Test	$-55 \sim +150^\circ C$, 30 minutes each	730	10 cycles	0	580	10 cycles	0
Resistance to Soldering Heat Test	$260^\circ C$, 10 seconds	22	—	0	22	—	0
Drop Shock Test	1500G, 0.5ms, XYZ(3 times each)	77	—	0	77	—	0
Vibration Fatigue Test	60Hz, 20G, XYZ(32 hours each)	38	—	0	38	—	0
Vibration-Variable Frequency Test	100~2000Hz, 20G, cycle time 4 min. XYZ (3 times each)	38	—	0	38	—	0
Constant Acceleration Test	20000G, XYZ(1 minute each)	38	—	0	38	—	0
Capability Against Electrostatic Discharge Test	$C=200pF$, $V=300V$ forward and reverse polarity between G-S (one time each)	100	—	0	100	—	0

Table 3-3 Changes of Major Parameters

Type No.	2SK135	Changes of breakdown voltage and saturation voltage	
Test item	High temperature reverse bias test		
Test condition	$T_a = 150^\circ\text{C}$ $V_{bsx} = 160\text{ V}, V_{GS} = -10\text{ V}$		
Failure criteria	V_{bsx} = higher than 128 V $V_{bs(sat)}$ = lower than 14.4 V $\Delta V_{bs(sat)}$ = within $\pm 30\%$		
Failure mode	Surface degradation		
Description			
1. There is almost no breakdown voltage change after 2,000 hours.			
2. Change of $V_{bs(sat)}$ increases a little at the initial period, but the changes is completely saturated after 2,000 hours.			
3. There is almost no degradation of V_{GS} , I_{DSS} and other parameters.			

4. Application Hints

4.1 Design of High Power Application (Parallel Operation)

As stated in section 3.5, the negative temperature coefficient of drain current and the high input impedance of power MOS FETs enable parallel operation to be performed with an extremely simple circuit.

In the parallel operation of bipolar power transistors, scattering of V_{BE} and h_{FE} characteristics causes an unbalance in collector current and, as a result, large current transistors generate high heat, which in turn further increases current flow; this may lead to thermal runaway. In a power MOS FET there is no possibility of thermal runaway because the drain current has a negative thermal coefficient.

Fig. 4-1 shows a triple connection circuit. Forward transfer admittance is three times as large as when a single device is used. In Figs. 4-2 and 4-3, this is expressed in waveform on a curve tracer. A current of about 20 A can be controlled by several volts of gate voltage.

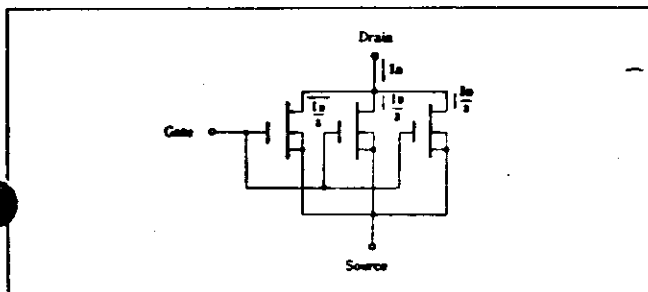


Fig.4-1 Triple Connection Circuit (Example of the N-Channel Device)

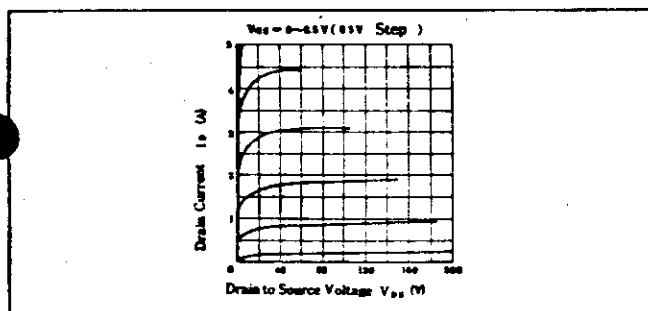


Fig.4-2 Output Characteristics in Triple Connection Circuit(1)

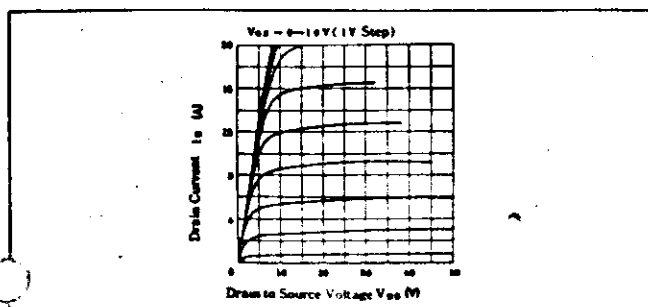


Fig.4-3 Output Characteristics in Triple Connection Circuit(2)

4.2 Design of High Breakdown Voltage Application (Series Operation)

(1) Totem pole connection

Fig. 4-4 shows a basic "totem pole" circuit, in which power MOS FETs are connected in series. This circuit has been used extensively as a saturated logic circuit, the basic circuitry for TTL IC. Operation of this circuit will be explained.

When no bias is applied to Q_1 , Q_1 is cut off because power MOS FETs have enhancement type transfer characteristics; thus the following relationships hold;

$$V_{G1} = 0, \quad I_D = 0$$

$$V_{G2} = \frac{1}{2}V_{DD} \quad (\because V_{G2} = V_{DD} \cdot \frac{R_g}{R_g + R_g})$$

$$V_O = V_{G2} - V_{GS2} \\ = \frac{1}{2}V_{DD} - V_{th2}$$

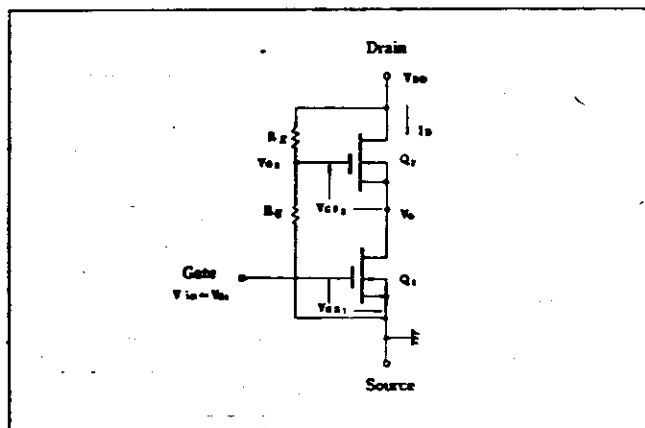


Fig.4-4 Basic Totem Pole Circuit

where V_{th2} is the threshold voltage of Q_2 . Generally, $V_{th2} < V_{DD}$. Therefore $V_O \approx \frac{1}{2}V_{DD}$.

And the voltage applied to Q_1 and Q_2 will be about $\frac{1}{2}V_{DD}$.

Next, let us consider a transient state. When the gate bias of Q_1 is increased gradually from zero, Q_1 will become conductive and so will Q_2 at the same time. If load resistance Z_L is inserted between V_{DD} and drain of Q_2 , drain voltage will be $V_D = V_{DD} - Z_L \cdot I_D$ and $V_O (= \frac{1}{2}V_D - V_{GS2})$ will gradually decrease.

If V_{DD} has a much larger value than V_{GS2} and Q_2 is driven up to the saturation region, then the characteristics of an equivalent MOS FET would be dependent on Q_1 .

Generally, when devices are operated in series, voltage unbalance due to switching time difference presents a problem. This problem is overcome in power MOS FETs because switching time can be made as short as several tens of nanoseconds.

Figs. 4-5 and 4-6 show breakdown and output characteristics where a single device is used. When this device is used in the circuit shown in Fig. 4-4, the breakdown and output characteristics would be as shown in Figs. 4-7 and

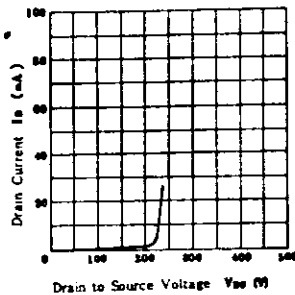


Fig. 4-5 Breakdown Characteristics (Single Device)

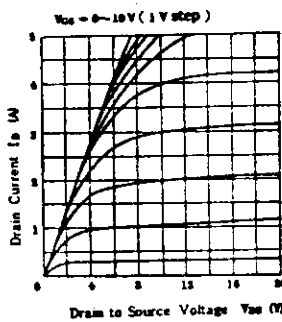


Fig. 4-6 Output Characteristics (Single Device)

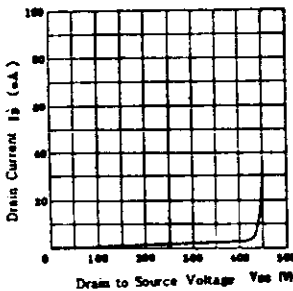


Fig. 4-7 Breakdown Characteristics

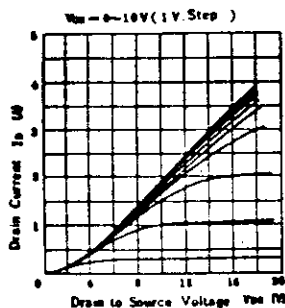


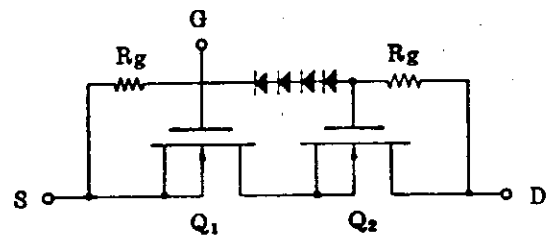
Fig. 4-8 Output Characteristics

4-8. Breakdown voltage in Fig. 4-7 is twice as high as in Fig. 4-5. The disadvantage is that on-resistance is also doubled, as is obvious from Figs. 4-8 and 4-6. A method of improving on-resistance is described in the following section.

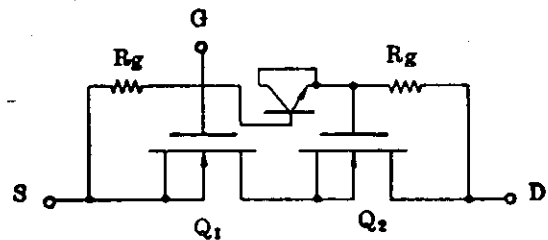
(2) How to reduce on-resistance in basic circuit

On-resistance (or saturation voltage) can be reduced by performing level shift of the Q_2 gate potential in the positive direction. This can be accomplished, for instance, by the methods shown in Fig. 4-9. Fig. 4-10 shows the output characteristics for a case where the gate is level-shifted to the positive side. (14 V is the maximum allowable gate-to-source voltage.)

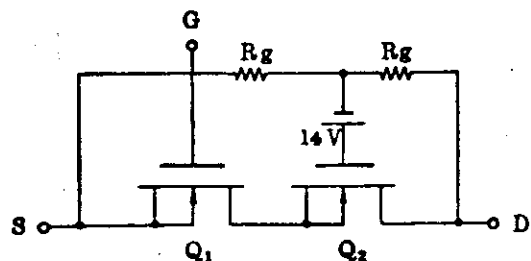
In the circuit shown in Fig. 4-9, as in the basic circuit, the equivalent drain to source breakdown voltage is twice as high as when a single device is used.



(A) Level Shift by Using of Diode



(B) Level Shift by Using of Breakdown Voltage in External Transistor



(C) Level Shift by Using of External Power Supply

Fig. 4-9 How to Reduce ON-Resistance

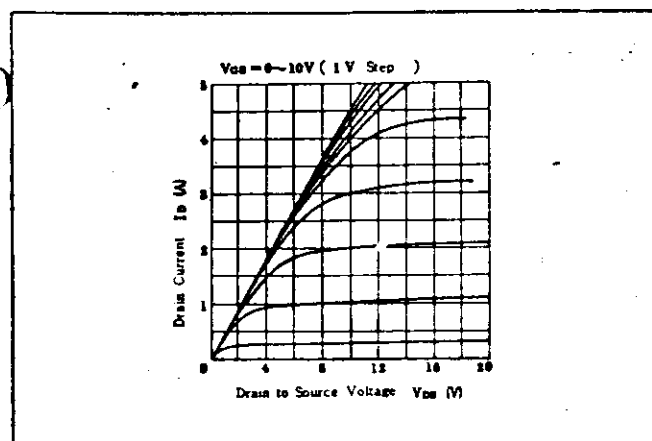


Fig. 4-10 Output Characteristics ((C) Circuit)

(3) Improvement of high frequency characteristics in totem pole connection

When the circuit shown in Fig. 4-4 is modified for a source follower, because of the different operation of Q_1 and Q_2 , a phase differential occurs under the influence of the power MOS FET input capacitance (about 500 pF for 2SK134, 600 pF for 2SJ49, $f=1$ MHz). As a result, characteristics worsen, as high frequency gain drops and phase shift increases.

This is expressed in Fig. 4-11. The equivalent circuit with passive devices alone is represented in Fig. 4-12.

It has been verified experimentally that the phase differential of V_{O1} and V_{O2} can be eliminated and driving in the same phase can be achieved by equalizing C_g with C_{in2} and that phase shift as 100 kHz can be limited within -90 degrees.

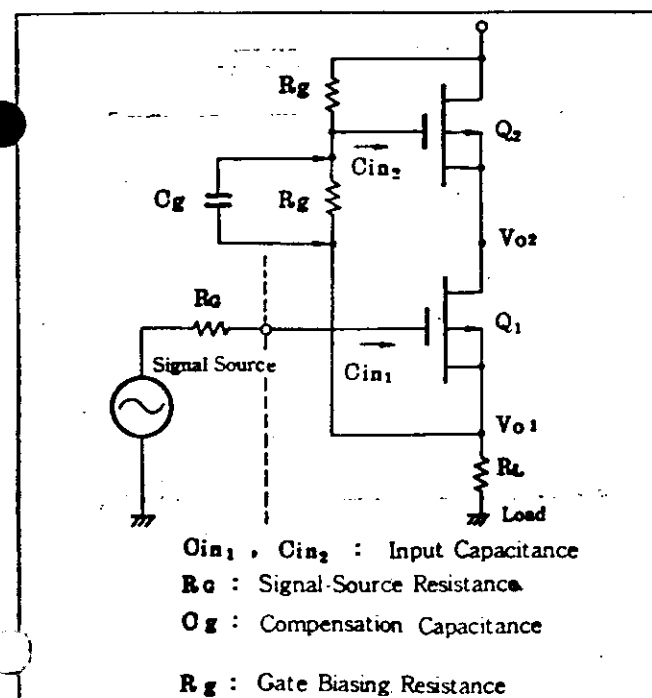


Fig. 4-11 Improved Totem Pole Circuit

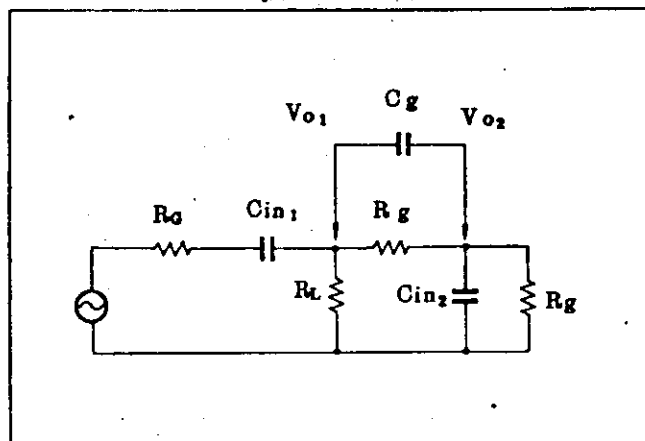


Fig. 4-12 Passive Equivalent Circuit of Totem pole

5 Reference Data

5.1 A.S.O. Limitation of Power MOS FETs

The most basic and important characteristic required of power device is a high breakdown strength. As stated, breakdown strength is closely related to other characteristics. Power MOS FETs have a thermal durability close to their thermal limitation, which is dependent on package configuration.

Fig. 5-1 shows breakdown points of power MOS FETs in relation to those of bipolar transistor. In Fig. 5-1, the curves marked 50, 100, 200, and 500 (W) are thermal limitation curves. Breakdown points of actual devices are along these curves.

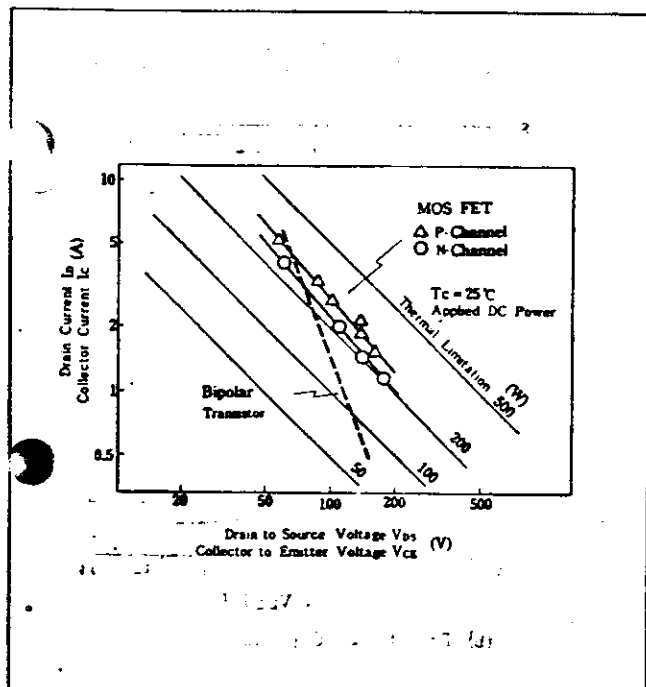
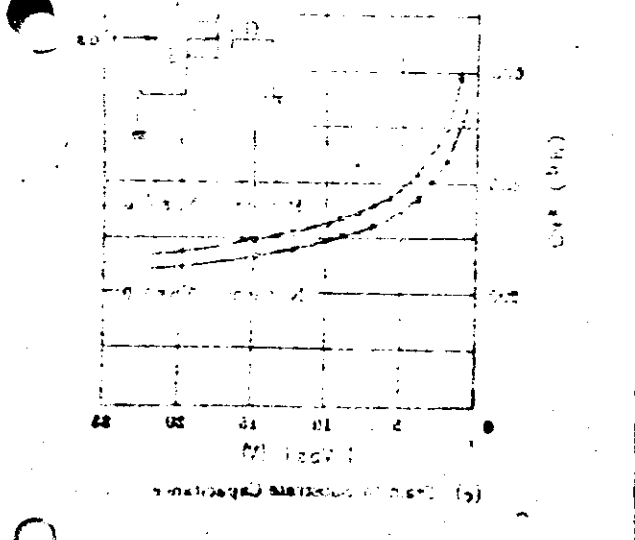


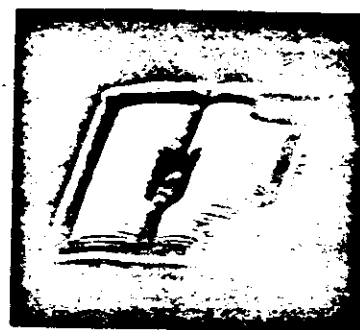
Fig.5-1 A.S.O. Limitation of Power MOS FET



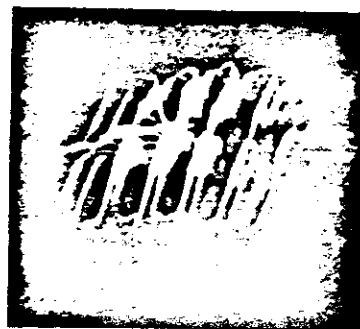
5.2 Thermal Mapping of Chip Surface Under Power Application

Current flowing in power MOS FETs does not concentrate locally but flows uniformly in the silicon chip.

Fig. 5-2 shows the thermal mapping of chip surfaces under power application for a power MOS FET and conventional bipolar transistors. Whereas the thermal mapping in the power MOS FET is uniform, a hot spot is generated in the bipolar transistor shown in Fig. 5-2 (c) although the power applied is one-half that applied to the power MOS FET.



$V_{ds} = 60V$, $I_d = 2A$
(A) Power MOS FET (2SK135)



$V_{ds} = 30V$, $I_d = 4A$
(B) Bipolar Transistor (2SC1343)

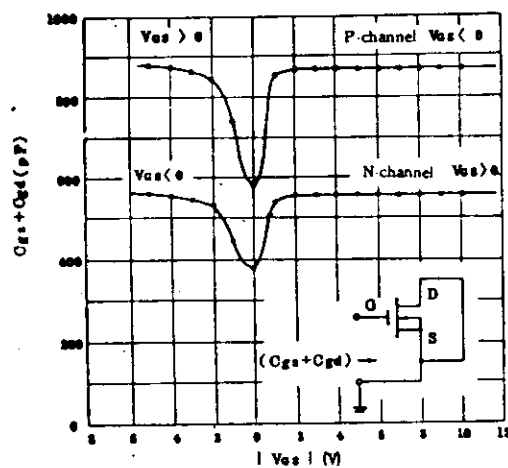


$V_{ds} = 60V$, $I_d = 1A$
Occurrence of Hot Spot
(C) Bipolar Transistor (2SC1343)

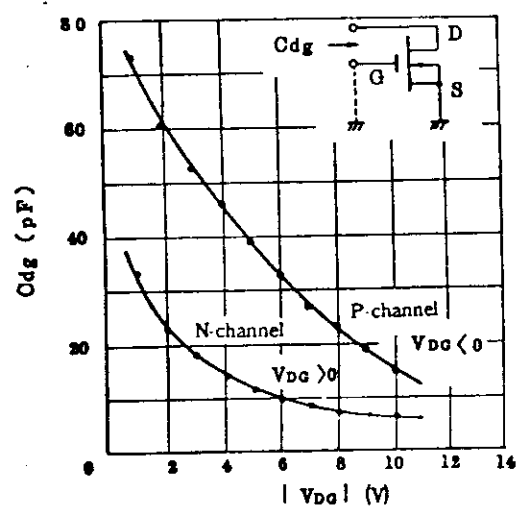
Fig.5-2 Thermal Mapping of Power MOS FET and Bipolar Transistor with an Infrared Scanner.

5.3 Input/Output Capacitance

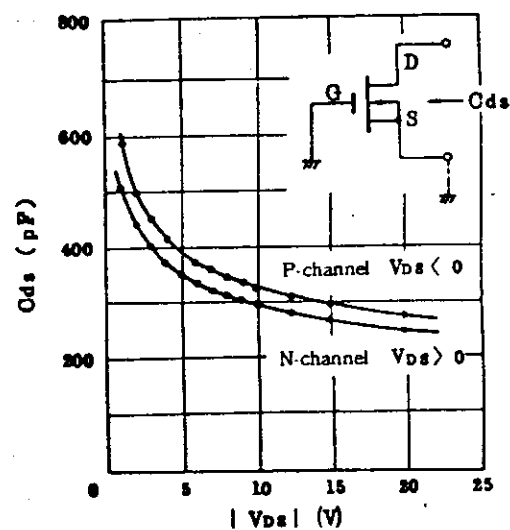
Fig. 5-3 (a), (b), (c) show the voltage dependence of electrode-to-electrode capacitance of power MOS FETs.



(a) Gate to Source Capacitance + Gate to Drain Capacitance



(b) Drain to Gate Capacitance



(c) Drain to Substrate Capacitance

Fig. 5-3 Bias Voltage Dependencies of Capacitance (2SK135/2SJ50)

6 Handling Precautions

Handling precautions and simple checking methods will be described for the benefit of those who use Hitachi's power MOS FETs.

If handled improperly, power MOS FETs cannot display their excellent performance described in the foregoing. Not only that. Improper use can lead to destruction of the devices.

Also, it is necessary to take into consideration the abnormal oscillation due to high gain, high input impedance, and excellent high frequency characteristics, which are some of the features of power MOS FETs.

By observing these precautions, circuits can be designed with outstanding performance that cannot be expected from using conventional power devices,

6.1 Pin Arrangement

As shown Fig. 6-1, the pin arrangement is different from that of ordinary transistors. (The source is the case.)

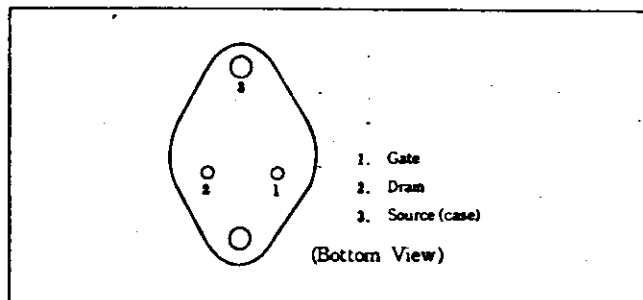


Fig.6-1 Pin Arrangement of Power MOS FET

6.2 Measurement of Breakdown Voltage V_{DSX} and V_{GSS}

Avoid measuring V_{DSX} (drain-to-source breakdown voltage) and V_{GSS} (gate-to-source breakdown voltage). At breakdown, negative resistance characteristics are generated, leading to oscillation and destruction.

6.3 Observation of I_D - V_{DS} Characteristics

- When the I_D - V_{DS} characteristics (source common output characteristics) are observed, oscillation may be caused depending on the type of curve tracer used (input capacity/resistance differs). This can lead to destruction of the device. Oscillation can be prevented effectively by connecting a series resistance of about 10 k Ω to the gate.
- When drawing a I_D - V_{DS} curve on an X-Y recorder, also, prevent oscillation by connecting a series resistance of about 10 k Ω to the gate or by inserting a capacitor of about 0.5 μ F between the gate and source.

6.4 Circuit Experiments

- In performing circuit experiments, it is recommended that you connect a resistance of 100 Ω ~ 2 k Ω to the gate in series, to prevent oscillation, until you get used to handling.
- In using the device as a source follower, it is recommended that oscillation be prevented by inserting a 100 μ F capacitor between the V_{DD} line near the drain and ground.

(Note)

The precautions described in 6.2 through 6.4 above are required because of the excellent high frequency characteristics and transfer characteristics of power MOS FETs.

6.5 Checking with Circuit Tester

Here are some simple ways to check power MOS FETs with a circuit tester to see that they operate normally.

- Gate-to-source

Check and make sure there is no gate-to-source conduction in either direction.

- Drain-to-source (for N-channel devices)

Set the circuit tester for resistance measurement ($\times 1\Omega$). As in Fig. 6-2 (a), connect the plus lead to the source, contact the minus lead to the gate and then connect it to the drain. Since the gate is then charged positively (forward biasing), the pointer will flip to indicate conduction.

Next, as in Fig. 6-2 (b), connect the minus lead to the source and after contacting the plus lead to the gate (whereupon the gate will be charged negatively), connect the minus lead to the drain and the plus lead to the source. The pointer will not flip indicating a cut-off state.

As long as the above results are obtained, the device may be expected to perform normally.

For P channel devices, checking can be performed similarly simply by reversing the plus and minus leads.

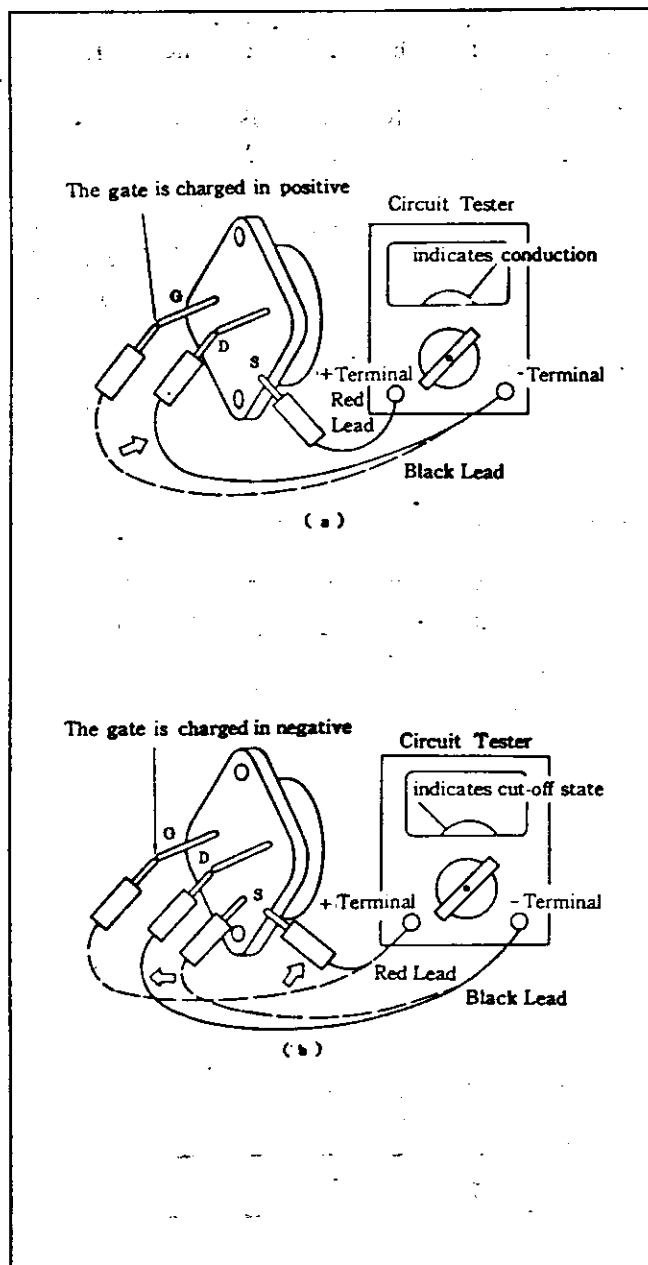


Fig.6-2 Checking with Circuit Tester for N-Channel Devices

Function		Application
Wide band linear amplification		<ul style="list-style-type: none"> • Audio power amplifiers* • Deflection circuits for CRT displays • Medium wave – high frequency band modulators, transmitters* • Citizen band transmitters
Power switching		<ul style="list-style-type: none"> • DC-AC inverters • AC-AC converters • DC-DC converters* • General-purpose switching regulators* • Pulse motor drivers
Power oscillation	Power application	<ul style="list-style-type: none"> • Humidifiers, cleaners and other ultrasonic applications* • High-frequency heaters*
	High voltage application	<ul style="list-style-type: none"> • Lighting equipment and other high frequency, high efficiency applications • Dischargers, air cleaners*
High-speed switching		<ul style="list-style-type: none"> • Laser pulsers • Modulators and drivers in high power transmitter circuits for optical communication • Bubble memory drivers
Other		<ul style="list-style-type: none"> • Series regulators

* Explained in detail in the following section.

8 Designing Application Circuits

8.1 Audio Power Amplifiers

Basic design philosophy

• Frequency characteristics (frequency vs. gain, phase)

The output stage of an ordinary power amplifier uses a push-pull emitter follower (source follower). This method is popular because it provides a wider transfer bandwidth and more stable operation than other grounding systems.

Meanwhile, the forward transconductance (forward transfer admittance) y_{fs} of power MOS FETs is as large as 1.0 S (siemens). Yet it is only a fraction of that of general bipolar transistors and this represents a disadvantage in terms of open loop distortion. The reason is that when bipolar transistors are used as an emitter follower, y_{fs} is given as:

$$y_{fs} = 1/r_e = \frac{I_E}{KT/q}$$

where r_e = Emitter equivalent resistance

K = Boltzmann constant

T = Absolute temperature

q = Electron charge

I_E = Emitter bias current

R_L = Load resistance

Even when I_E is 1 A, for instance, $y_{fs} \approx 40$ S.

Now the relationship between input and output is

$$e_o/e_i = \frac{R_L}{R_L + 1/y_{fs}}$$

and the nonlinear component of y_{fs} causes distortion, so that a larger y_{fs} is of greater advantage. In other words, since a power MOS FET has a distortion about 20 dB larger than a bipolar transistor, it is necessary to use a larger open loop gain and a larger negative feedback than a bipolar transistor. As shown by the frequency characteristics in Fig. 3-4, however, a Darlington connection must be used for bipolar transistors in order to enlarge the bandwidth, so that the two-stage emitter follower would worsen the phase characteristics. In applying a negative feedback, a large phase shift would force a sacrifice of gain frequency characteristics in a phase compensation circuit and the like. Thus, with a source follower with a single power MOS FET, much feedback can be applied over a large bandwidth, and distortion can be reduced.

The driver stage of a power MOS FET does not require a conventional class B driver stage. Therefore, the poles in the amplifier system can be reduced. A stable negative feedback amplifier can be formed.

In the frequency characteristics of open loop gain, setting the peak value near 10 ~ 20 kHz is the key

to forming a good circuit.

Setting the peak value at the upper limit of the audible range is impossible with conventional bipolar transistors. This can be realized only by using power MOS FETs with excellent high-frequency and switching characteristics.

Fig. 8-1 shows the difference in open loop gain of audio amplifiers designed with power MOS FETs and bipolar transistors.

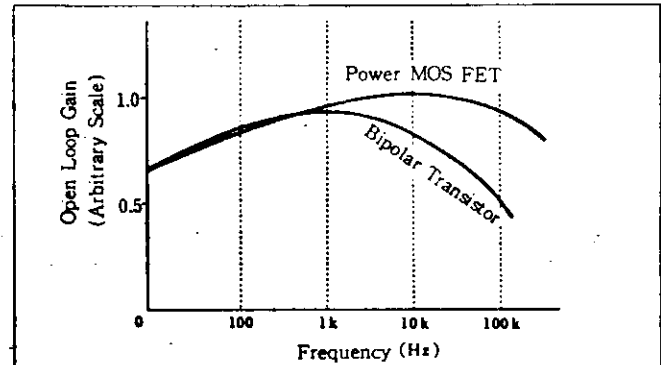


Fig.8-1 Open Loop Gain of Audio Power Amplifier

• Consideration for parasitic oscillation

As power MOS FETs have excellent high-frequency characteristics, they are liable to cause oscillation when used in high-gain designs such as described in the preceding section. To avoid this, a gate resistance (200 ~ 500 Ω) may be used to prevent a real part of the input impedance to be negative. Or the gate wiring pattern may be minimized (within 5 cm), as stated in the section on precautions in fabrication later in this manual. Or one-point grounding may be used.

When a gate resistance is inserted, frequency characteristics are worsened as shown in Fig. 8-2, so that optimum values must be selected in designing. The gate resistance will have no effect in case the former stage has a high impedance as in a class A driver stage.

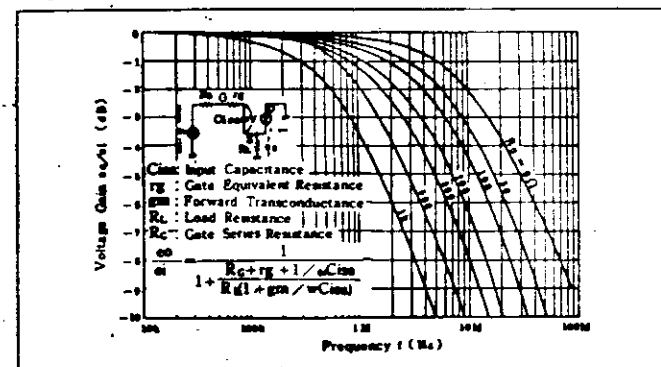


Fig.8-2 Frequency Characteristics of Source Follower. (Calculated Value)

(2) Typical design — 1 (100 W output at 100 kHz, 0.01%)

A circuit is shown in Fig. 8-3. Design of each amplifier stage will be discussed below.

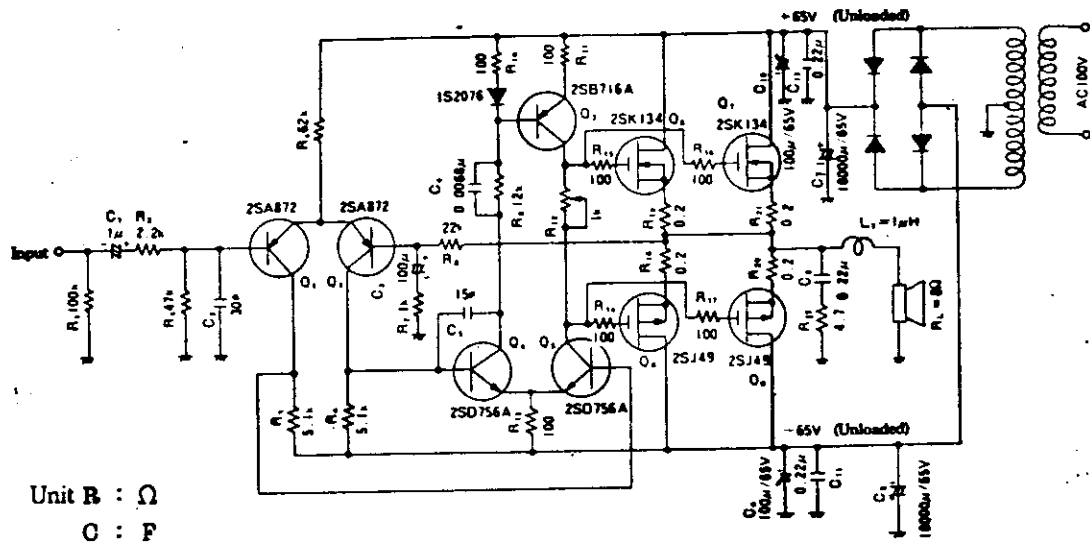


Fig. 8-3 Full Circuit of 100 W Output Audio Amplifier

Design of output stage

Fig. 8-4 shows an equivalent circuit of the output stage for N channel MOS FETs. R_{ON} is a drain-to-source equivalent resistance when the power MOS FET is on. The resistance 1.71Ω contains some margin as it was calculated for the worst case from the specifications for 2SK135 and 2SJ50.

$$R_{ON} = \frac{V_{DS(sat)}}{I_D} = \frac{12}{7} \approx 1.71 (\Omega)$$

Peak current I_p flowing in load $R_L = 8 \Omega$ at $P_O = 100 \text{ W}$ is calculated from mean current I ,

$$P_O = I^2 \cdot R_L, I_p = \sqrt{2} \cdot I,$$

$$\text{as } I_p = \sqrt{2} \cdot \sqrt{\frac{P_O}{R_L}} = \sqrt{2} \cdot \sqrt{\frac{100}{8}} \approx 5 \text{ A.}$$

Therefore, if transformer regulation is estimated as 20% and AC line regulation as $\pm 15\%$, then power supply voltage V_{DD} is given as

$$V_{DD} = 1.2 \times 1.15 \{R_L + 0.5(R_{ON} + R_S)\} \times I_p \approx 61.8 \text{ V.}$$

In Fig. 8-3, the voltage is set at $\pm 65 \text{ V}$ including a margin.

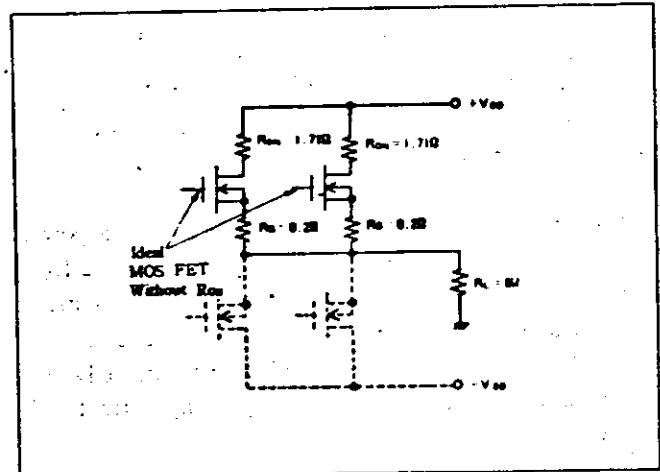


Fig. 8-4 Equivalent Circuit of the Output Stage for N-Channel Power MOS FETs

• Design of voltage amplifier stage

A power MOS FET can be used with a low driving power. Fundamentally, only the power for charging and discharging the gate-to-source capacitance is needed to the output stage, so that no class B driver stage is required.

The driving power varies with input frequency. At 100 W output and 10 kHz frequency, it would be about 10 mW.

Therefore, an output stage power MOS FET can be driven directly from a class A predriver (voltage amplifier stage) used in a bipolar transistor amplifier. By eliminating the class B driver, the number of components can be reduced, and impairing the amplifier's performance caused by the driver itself can be avoided. Further, the number of poles for transfer function (open loop gain vs. frequency characteristics) decrease, and the stagger can easily be increased. Consequently, the stability against oscillation is improved.

Transistors for the voltage amplifier stage are required to have a high voltage durability, low C_{ob} , and high f_T . Here the 2SD756A/2SB716A developed especially for power MOS FETs are used. With the NPN differential amplifier and PNP constant current load, high gain and low distortion characteristics were obtained.

The class A stage bias current is set as 10 mA. When bias current is lacking, sufficient power to drive a power MOS FET at high frequency cannot be supplied, and distortion would worsen.

The drain current temperature coefficient of a power MOS FET undergoes a reversal of polarity at around $I_D = 100$ mA and temperature compensation in the large current region will be unnecessary. Hence, the bias circuit for a power MOS FET is vastly simplified because only one fixed resistor (1 k Ω) for setting idling current will suffice.

• Design of input stage circuit

For the input stage, a stable differential amplifier circuit was formed by using the high-voltage, low-noise transistor 2SA872, which is known for its high performance in improving the S/N ratio. Bias current is set as 0.5 mA.

• Typical characteristics of experimental circuit (Fig. 8-3)

Output vs. distortion characteristics are shown in Fig. 8-5. At $f = 1$ kHz, total harmonic distortion (THD) is approximately 0.002%, which is the limit value for any measuring system available on the market today.

Through optimum design, the following can be obtained at rated output:

$$f = \text{DC} \sim 100 \text{ kHz},$$

$$\text{THD} \leq 0.01\%$$

Thus, characteristics that cannot be obtained with conventional bipolar transistors are realized with power MOS FETs.

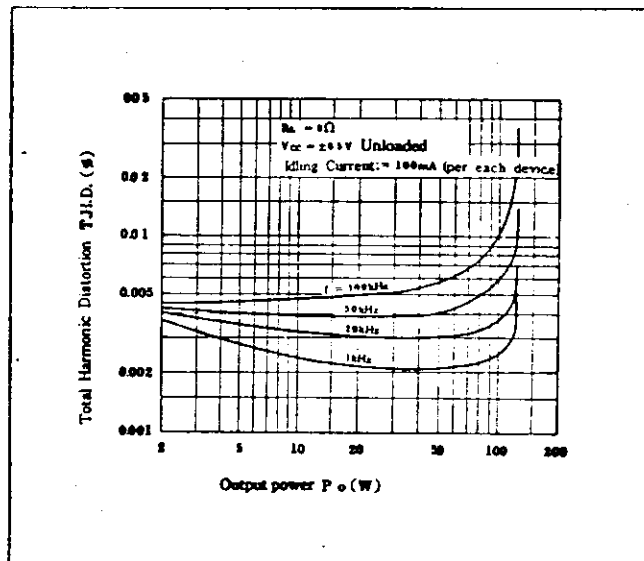


Fig.8-5 Total Harmonic Distortion VS. Output Characteristics

• Precautions in fabrication

- Minimize the gate wiring, although its relationship with gate resistance must be taken into consideration.
- Provide one-point grounding for the amplifier base plate, power supply, chemical capacitor to prevent \pm line unbalance, and speaker terminals.
- The output coupling coil has the effect of reducing distortion in the high frequency range, and preventing abnormal oscillation in capacitance loaded operation. But the values should be determined while experimenting.

Fig. 8-8 shows the standard printed pattern. The amplifier devices that drive the output stage power MOS FETs consist only of five small-signal transistors, so that the printed board is extremely small.

Wiring between the voltage amplifier stage collector and the power MOS FET gate must be minimized. The arrangement and configuration of the printed board and the heat sink must be selected carefully.

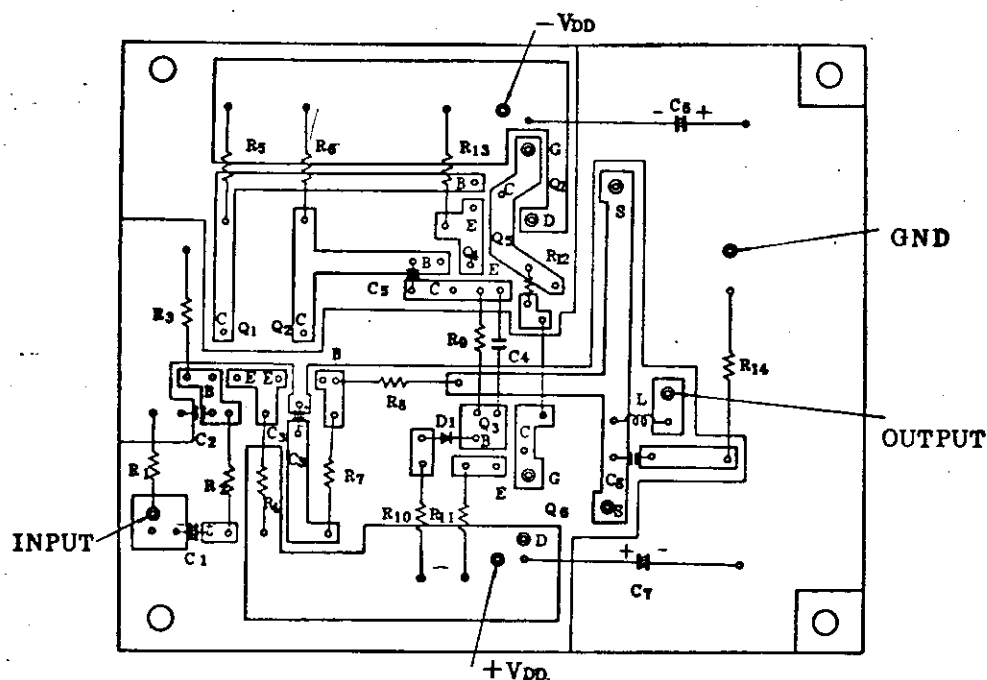


Fig.8-8 Standard Printed Pattern in Actual Size

In Fig. 8-8 which shows the example of the printed board pattern, the printed board is attached directly to the heat sink to minimize the gate wiring.

(4) Recommended line-up by output power

Line-up of devices in audio amplifiers of different outputs is shown Table 8-1.

Table 8-1 Line-up of Devices in Audio Power Amplifier

Output Power (W)	Input Stage		Driver Stage		Output Stage					
	N-Channel (NPN)	P-Channel (PNP)	N-Channel (NPN)	P-Channel (PNP)	Con- nection	TO-3		HPAK		V _{DSX} (V)
						N-Channel	P-Channel	N-Channel	P-Channel	
50~80	2SK151 (TO-92MOD.)	2SJ51 (TO-92MOD.)	2SK213 (TO-220AB)	2SJ76 (TO-220AB)	Single Push-Pull	2SK133	2SJ48	2SK225	2SJ81	120
	2SC1775 (TO-92)	2SA872 (TO-92)	2SD756 (TO-92MOD.)	2SB716 (TO-92MOD.)						
			2SD756A (TO-92MOD.)	2SB716A (TO-92MOD.)		2SK134	2SJ49	2SK226	2SJ82	140
			2SK214 (TO-220AB)	2SJ77 (TO-220AB)						
100~140	2SC1775 (TO-92)	2SA872 (TO-92)	2SD758 (TO-202AA MOD.)	2SB718 (TO-202AA MOD.)	Parallel Push-Pull	2SK175	2SJ55	—	—	180
			2SK216 (TO-220AB)	2SJ79 (TO-220AB)						
			2SD666A (TO-92MOD.)	2SB646A (TO-92MOD.)		2SK134	2SJ49	2SK226	2SJ82	140
			2SK214 (TO-220AB)	2SJ77 (TO-220AB)						
			2SD668A (TO-126MOD.)	2SB648A (TO-126MOD.)		2SK135	2SJ50	2SK227	2SJ83	160
			2SK215 (TO-220AB)	2SJ78 (TO-220AB)						
150~200	2SC1775A (TO-92)	2SA872A (TO-92)	2SD758 (TO-202AA MOD.)	2SB718 (TO-202AA MOD.)		2SK176	2SJ56	—	—	200

8.2 Power Oscillators (I)

Power MOS FETs have excellent high frequency characteristics and their operating frequency extends to the 10 MHz band and higher. Taking advantage of their high switching speed and ease of biasing, one can use them for economical high-frequency power sources as in such new application as high-frequency heating and high voltage generation.

Power MOS FETs require a far lower driving power than bipolar transistors do, and can be parallel-operated easily, providing the required large output. Basic design procedures for an oscillation circuit and practical applications will be described below.

(1) Basic design of power oscillation circuit

Operation in a high frequency circuit is affected by light capacitances of the devices and parts used. Also, depending on the DC bias circuit arrangement and ground points, feedback quantity varies and affects the characteristics. Therefore, a circuit configuration determined through calculations must be modified in the process on construction. Described below are the basic principles that provide design guidelines for high frequency FET oscillation circuits.

In Fig. 8-9, (a) is a basic oscillation circuit, and (b) an equivalent circuit. Z_1 , Z_2 and Z form a tank circuit. By using the same type of reactance for Z_1 and Z_2 , positive feedback can be applied. The signal applied to the gate is amplified at the drain with a 180° phase differential and current of the same phase flows in reactances Z_1 and Z_2 , so that it will have a 180° phase differential against the source current. As a result the amplified signal at the gate is positively fed back.

When power MOS FETs are used in a Colpitts oscillation circuit with Z_1 and Z_2 as capacitances, operation at high frequency becomes possible.

Limitation for high frequency operation is created by losses expressed by electrode capacitance C_{gs} and series gate resistance R_g in Fig. 8-9. The voltage applied to the gate is divided between R_g and C_{gs} , and reduces g_m at high frequency. At the same time, phase delay is caused.

The frequency at which g_m decreases by about 3 dB is, in the case of 2SK135:

$$f_{(3dB)} = \frac{1}{2\pi \cdot R_g \cdot C_{gs}} \\ \approx 3 \text{ MHz}$$

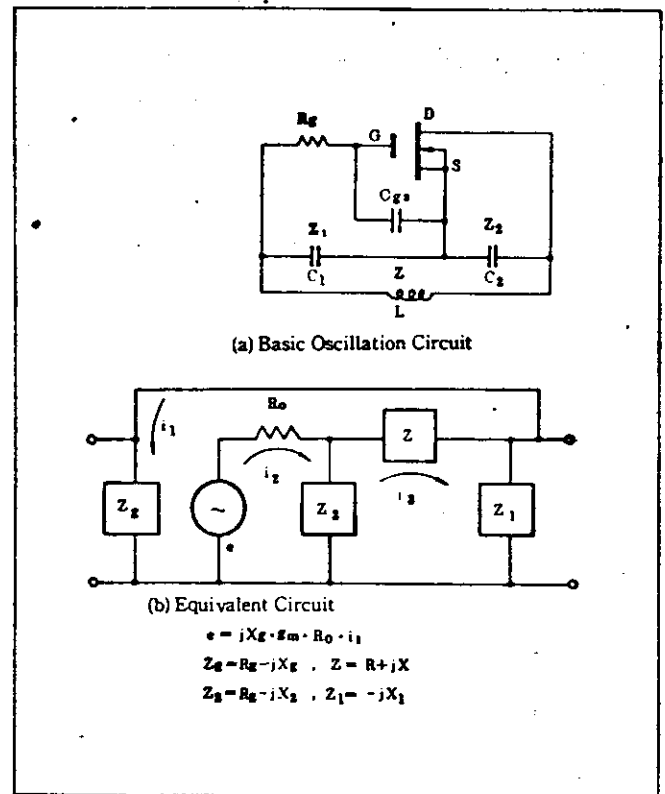


Fig.8-9 Basic Oscillation Circuit and Equivalent Circuit by Using a Power MOS FET

• Oscillating conditions

Since power MOS FETs have a large g_m and power gain, an oscillator can be formed even at frequencies higher than $f_{(3dB)}$.

Next, oscillating conditions will be sought for Fig. 8-9 (b).

When gate current is denoted by i_1 , drain current by i_2 , and tank circuit current including load by i_3 , the following equation holds for the loop current:

$$\left. \begin{aligned} -jX_g \cdot g_m \cdot R_o \cdot i_1 + (R_o + Z_2) i_2 - Z_2 \cdot i_3 &= 0 \\ Z_1 \cdot i_1 + Z_2 \cdot i_2 - (Z_2 + Z + Z_1) i_3 &= 0 \\ (Z_1 + Z_g) i_1 - Z_1 \cdot i_3 &= 0 \end{aligned} \right\} \dots\dots\dots (1)$$

Equation (1) has finite solutions other than $i_1=i_2=i_3=0$. In other words, in order that the circuit may oscillate, it is necessary that the value of the determinant consisting of constants be zero, as follows:

$$\left. \begin{aligned} Z_2 (jX_g \cdot g_m \cdot R_o + Z_2 \cdot \frac{Z_1 + Z_g}{Z_1}) \\ - (R_o + Z_2) \left\{ Z_1 + \right. \\ \left. (Z_2 + Z + Z_1) \frac{Z_1 + Z_g}{Z_1} \right\} &= 0 \end{aligned} \right\} \dots\dots\dots (2)$$

In an area of operation where drain current i_2 is not dependent on drain voltage but rather on gate voltage, R_o is far larger than the other parameters and the following equation holds:

$$jZ_2 \cdot X_g \cdot g_m + Z_1 - (Z_2 + Z + Z_1) \frac{Z_1 + Z_g}{Z_1} = 0 \quad (3)$$

The imaginary part is:

$$R_2 \cdot X_1 \cdot X_g \cdot g_m - (R_2 + R) R_g + (X_2 - X)(X_1 + X_g) + X_1 \cdot X_g = 0 \quad (4)$$

If the terms with load resistances R_2 and R of the oscillator are neglected, then frequency would be determined by the following equation:

$$X = \frac{X_1 \cdot X_g}{X_1 + X_g} + X_2 \quad (5)$$

Thus,

$$(2\pi f)^2 = \omega^2 = \frac{1}{L} \left(\frac{1}{C_1 + C_g} + \frac{1}{C_2} \right) \quad (6)$$

Next, from the real part, we get:

$$X_2 \cdot X_g \cdot g_m - (R_2 + R) \frac{X_1 + X_g}{X_1} - (X_2 - X + X_1) \frac{R_g}{X_1} = 0 \quad (7)$$

$$g_m - \frac{(R_2 + R)}{X_2^2} \cdot \frac{X_2}{X_1 \cdot X_g / (X_1 + X_g)} - \frac{R_g}{X_g^2} \cdot \frac{X_1 \cdot X_g}{X_1 + X_g} \cdot \frac{1}{X_2} = 0 \quad (8)$$

From Equation (8), since g_m must be large enough to compensate for circuit loss, the following oscillation start conditions are obtained:

$$g_m \geq \frac{C_2}{C_g + C_1} \cdot G_{in} + \frac{C_g + C_1}{C_2} \cdot G_L \quad (9)$$

Where G_{in} and G_L are loss conductances of input and output circuits respectively.

$$G_{in} \geq \frac{R_g}{X_g^2}, G_L \geq \frac{R_2 + R}{X_2^2}$$

In the case of high-efficiency power oscillators, the second term on the right side of Equation (9) represents an input loss term, and g_m is expressed with gate voltage V_g , output voltage V_{out} , and output power P_{out} , as follows:

$$g_m \geq \frac{V_{out}}{V_g} \cdot G_L = \frac{2 \cdot P_{out}}{V_g \cdot V_{out}} \quad (10)$$

• DC bias conditions and AC amplitude

Let us consider the relationship between DC bias conditions and AC amplitude in the various operating modes of the power oscillator in Fig. 8-10.

At conductor angle θ , the various current and voltage parameters of the device are as shown in Fig. 8.11. Drain current is:

$$i_D = I_A (\cos \omega t - \cos \varphi) \quad (11)$$

Basic wave amplitude:

$$I = \frac{2}{\pi} \cdot \int_0^\varphi i_D \cos \omega t d(\omega t) = I_A \cdot \frac{\varphi - \sin \varphi \cdot \cos \varphi}{\pi} \quad (12)$$

Mean current:

$$I_O = \frac{1}{\pi} \cdot \int_0^\varphi i_D d(\omega t) = I_A \cdot \frac{\sin \varphi - \varphi \cos \varphi}{\pi} \quad (13)$$

The relationship with peak current: $I_p = I_A (1 - \cos \varphi)$

$$I = I_p \cdot \frac{\varphi - \sin \varphi \cdot \cos \varphi}{\pi(1 - \cos \varphi)} \quad (14)$$

$$I_O = I_p \cdot \frac{\sin \varphi - \varphi \cos \varphi}{\pi(1 - \cos \varphi)} \quad (15)$$

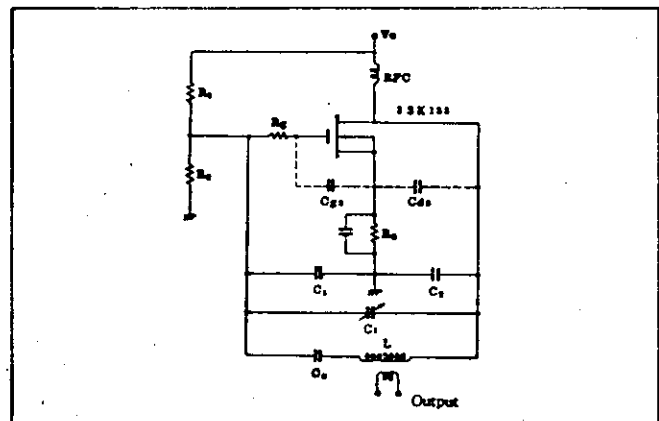


Fig.8-10 Colpitts Oscillation Circuit(Clap-Type)

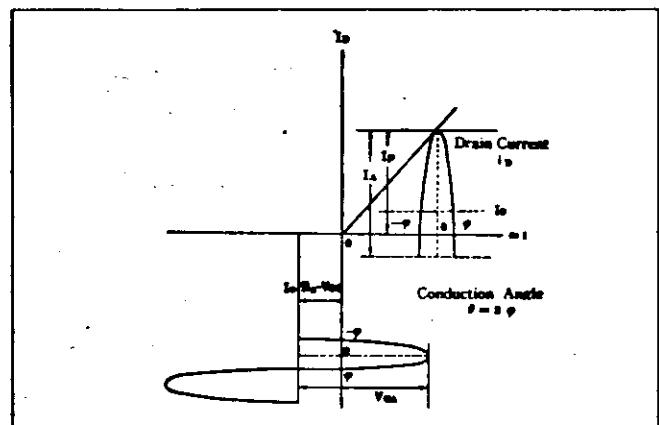


Fig.8-11 Operating Mode of Power Oscillator

The ratio of maximum power against supplied DC power, viz., drain efficiency, is expressed as follows, where current and voltage efficiencies are denoted by η_i and η_e respectively:

$$\eta_D = \eta_e \cdot \eta_i, \quad \eta_e = \frac{V}{V_O} \\ \eta_i = \frac{1}{2} \cdot \frac{1}{I_O} = \frac{1}{2} \cdot \frac{\varphi - \sin \varphi \cdot \cos \varphi}{\sin \varphi - \varphi \cos \varphi} \quad (16)$$

η_c can be calculated similarly.

The relationship between conduction angle θ and η_i is given as in Fig. 8-12.

Next, the bias conditions that determine conduction angle $\theta = 2\varphi$ will be sought.

If peak gate voltage is denoted by V_{GP} then:

$$V_{GP} = V_{GO} + V_{GA} - R_3 \cdot I_O \quad (17)$$

where $V_{GO} = V_O \cdot \frac{R_2}{R_1 + R_2}$: Initial bias voltage to gate

V_{GA} : Gate amplitude

I_O : Drain mean current

R_3 : Source resistance

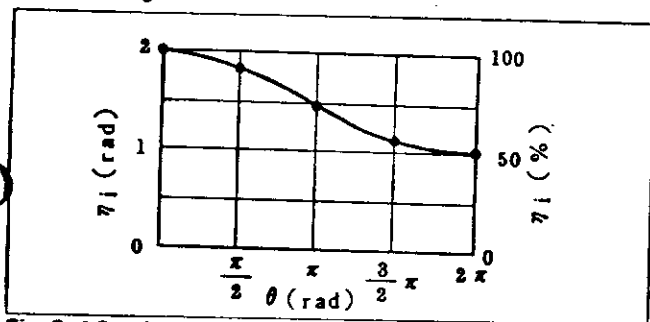


Fig. 8-12 Current Efficiency VS. Conduction Angle

If the gate voltage satisfying the conditions for oscillation start is

$$V_{GST} = V_{GO} - R_3 \cdot I_{ST} \quad (18)$$

then, from Fig. 8-11, we get

$$V_{GA} \cdot \cos\varphi = R_3 \cdot I_O - V_{GO} \quad (19)$$

From Equations (17), (18), (19), we get:

$$R_3 = \frac{V_{GST} + \frac{\cos\varphi}{1 - \cos\varphi} \cdot V_{GP}}{I_O - I_{ST}} \quad (20)$$

$$V_{GO} = V_{GST} + R_3 \cdot I_{ST} \quad (21)$$

$$V_{GA} = \frac{V_{GP}}{1 - \cos\varphi} \quad (22)$$

• Determination of circuit parameters

Circuit parameters and maximum ratings of devices for an FET oscillator will be considered. For high-efficiency operation, drain bias voltage must be maximized. Let us make it one-half the allowable voltage V_{DSX} max. of the device.

$$V_O = \frac{1}{2} V_{DSmax} \quad (23)$$

From the relationship between allowable drain loss and mean voltage, we get the drain mean current as follows:

$$I_O = \frac{P_D}{V_O} \quad (24)$$

Equation (24) represents a condition where allowable loss is not exceeded even at oscillation stop.

24. HITACHI

The peak current for class B operation is obtained from Equation (15) as follows:

$$I_p = \pi \cdot I_O \quad (25)$$

Gate peak voltage V_{GP} can be determined as a value corresponding to I_p in Equation (25) from the $I_D - V_{DS}$ characteristics of power MOS FETs (see Figs. 3-1 and 3-2 in Chapter 3). As for oscillation starting current I_{st} , from the conditions of Equation (10), denoting drain voltage amplitude by V , the following is determined:

$$g_m > \frac{2 \cdot P_{out}}{V_g \cdot V} = \frac{2 \cdot I_O \cdot \eta_p}{V_g} \quad (26)$$

For safety's sake, the value of oscillation start current is determined from the $g_m - I_D$ characteristics of power MOS FETs (see Fig. 8-13) as the value of I_{st} corresponding to twice the value of Equation (26). From these data and Equations (20), (21) and (22), the bias parameters of V_{GO} and V_{GA} can be determined.

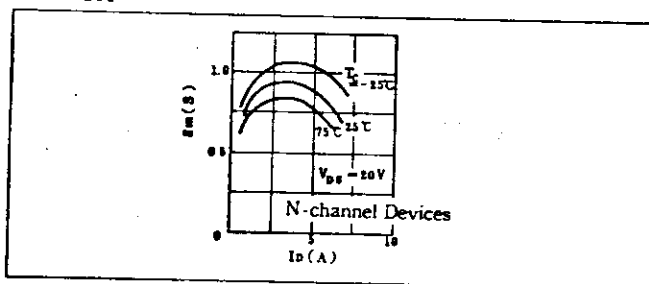


Fig. 8-13 Drain Current Dependency of Transconductance

• Example of parameter calculation

By applying the above method to 2SK135, the following calculated results are obtained:

$$\begin{aligned} V_O &= 70 \text{ (V)} \\ I_O &= 1.43 \text{ (A)} \\ I_p &= 4.5 \text{ (A)} \\ V_{GP} &= 6 \text{ (V)} \\ g_m &= 2 \times 0.374 \text{ (S)} \\ I_{st} &= 0.6 \text{ (A)} \\ V_{GO} &= 2.9 \text{ (V)} \\ V_{GA} &= V_{GP} = 6 \text{ (V)} \end{aligned}$$

• Calculation of resonator capacitance

In order to set the divided voltages of gate voltage $V_g (= V_{GA})$ and drain voltage V_D to meet the above operating conditions, resonator capacitances C_1 and C_2 will be determined.

With regard to drive voltage drop due to R_g , the following equation holds:

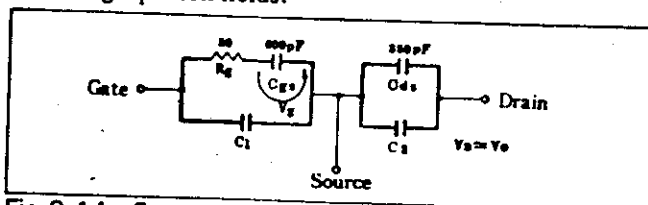


Fig. 8-14 Equivalent Circuit of Resonator

Fig. 8-18 plots output voltage and frequency with C_1 as parameter under the conditions of $C_1' = \infty$, $C_2 = 0.05 \mu\text{F}$, $L = 0.0384 \text{ mH}$, $C_S = 5 \text{ pF}$, $R_E = 2 \Omega$, $C_E = 0.1 \mu\text{F}$, $C_L = \text{Open}$, $R_2 = 70 \text{ k}\Omega$, $V_i = 45 \text{ V}$.

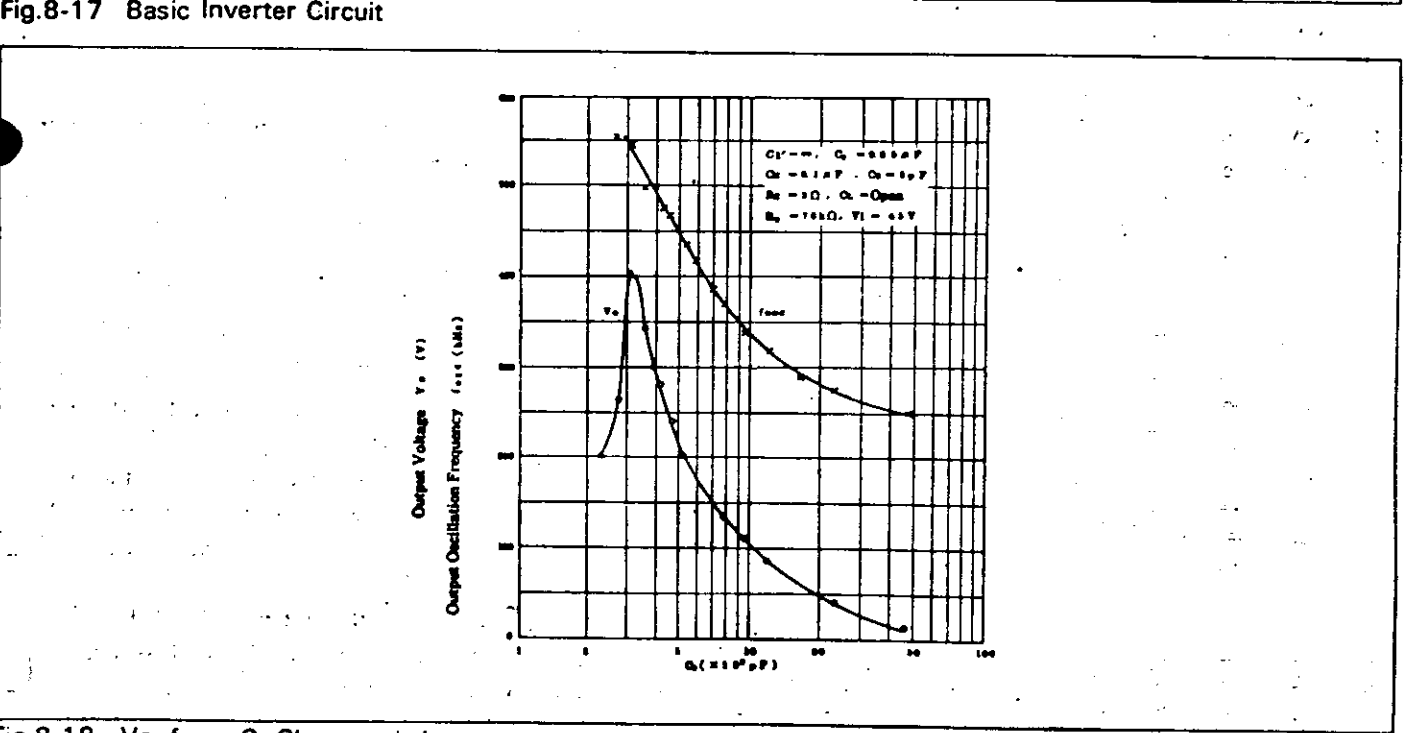
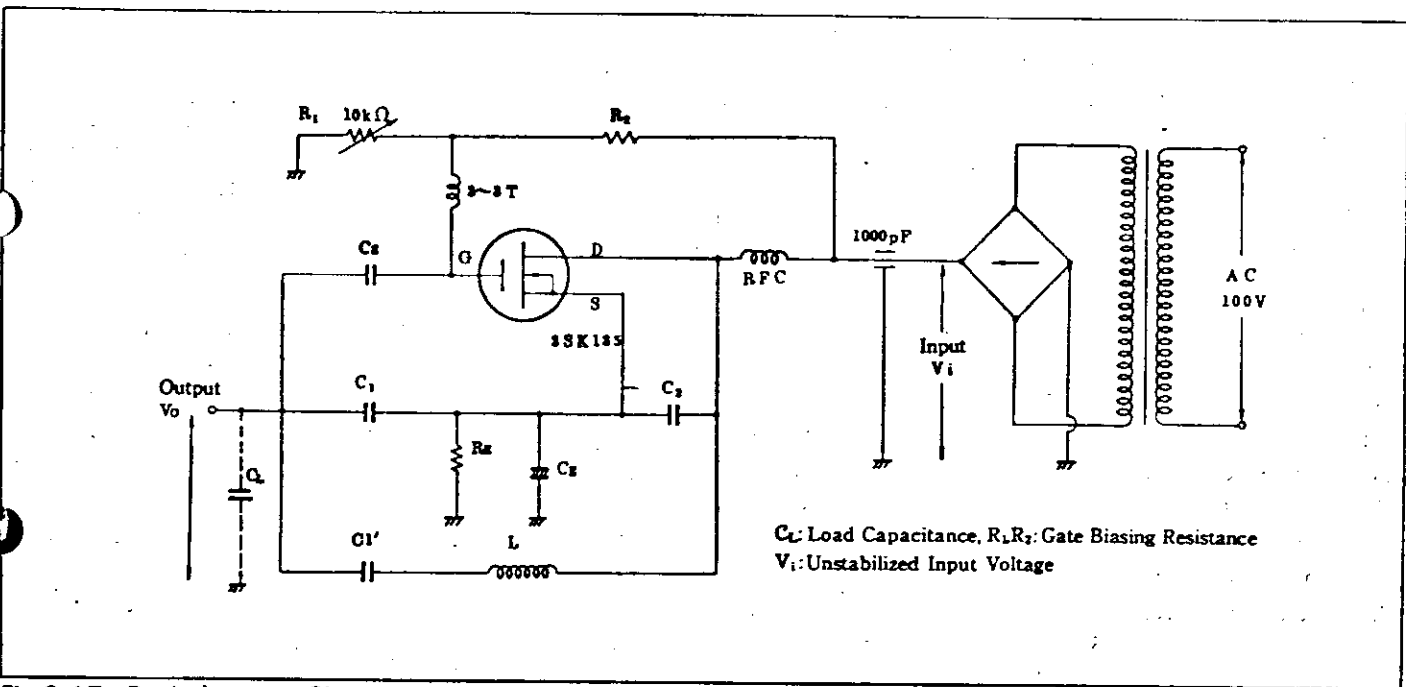
The figure shows that output voltage is dependent on the C_1 value and there is an optimum output voltage. Oscillation frequency also varies with C_1 and shows a tendency of monotone increase and decrease.

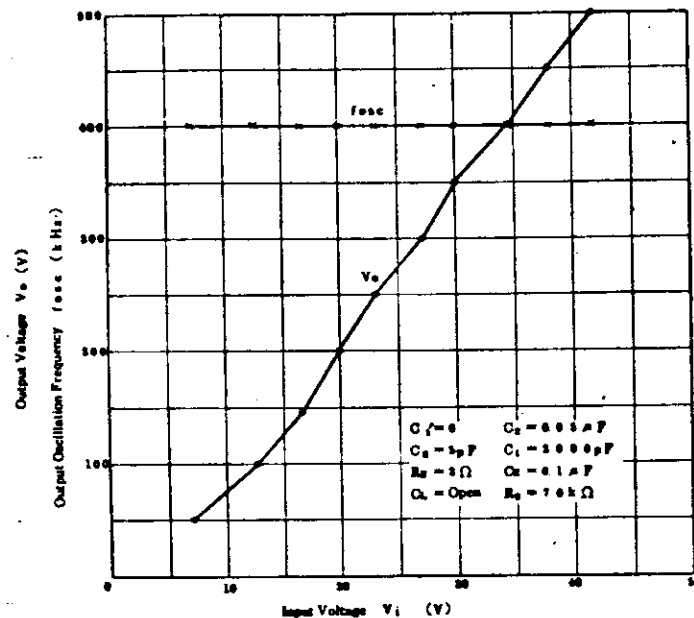
Next, characteristics measured with input voltage V_i as parameter are shown in Fig. 8-19. The measurement conditions are $C_1' = \infty$, $C_2 = 0.05 \mu\text{F}$, $C_S = 5 \text{ pF}$,

$R_E = 2 \Omega$, $C_E = 0.1 \mu\text{F}$, $C_L = \text{Open}$, $R_2 = 70 \text{ k}\Omega$.

Fig. 8-19 shows that the desired output voltage is dependent on input V_i and can be selected at will and that frequency variation can be reduced. Frequency drift during operation is due to heat generation in the capacitor. For practical purposes, a low-loss capacitor with a small temperature coefficient (e.g., mica, polypropylene) must be used.

The inverter introduced above involves a relatively small power. But a similar principle applies to high-voltage power supplies that require higher frequencies and higher voltages.



Fig.8-19 V_o , f_{osc} - V_i Characteristics

8.4 Medium-Wave Transmitters (Based on data of NHK Technical Research Laboratories)

Solid state devices are being used increasingly nowadays in medium-wave transmitters. However, no optimum power devices are available for use in power amplifier circuits and not a few problems involving circuit performance remain to be resolved. A high-efficiency, high-power pulse amplifier using power MOS FETs will be described.

Generally, in pulse amplification, power MOS FETs have many advantages over bipolar transistors, as follows:

- Pulse width does not change because of the absence of carrier storage effect.
- Drain current has a negative temperature coefficient, so that no thermal runaway or current hogging occurs; as a result, stable operation is ensured.
- They have a large input resistance; since they are enhancement type devices, input and output terminals are isolated and the bias circuit is simplified compared with other field effect transistors.
- A small driving power suffices; driver and input

power amplifier circuits are simplified.

- The desired output is obtained easily by parallel operation.
- Design, adjustment and operation are simple.

A class D SEPP pulse amplifier with 1 kW CW at 0.5 ~ 1.5 MHz carrier frequency and 80 ~ 90% overall efficiency will be described. A class D type is selected because a final power amplifier efficiency of 90% or better can be expected theoretically.

(1) Class D SEPP type pulse amplifier

Fig. 8-20 is a block diagram of the power amplifier.

In the carrier generator, radio frequency is pulse-width-modulated by the audio frequency signal. Here, pulse-width-modulated wave is generated according to the two-valued logic, and is drawn out as two-phase pulse and applied to the driver stage.

The input parts of the power amplifier are transformer coupled. Amplitude modulation wave is mixed and filtered in the output tank circuit and applied to the load (antenna).

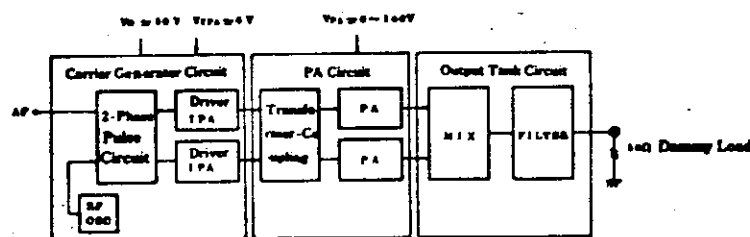


Fig.8-20 Block Diagram of SEPP Pulse Power Amplifier

Power amplifier circuit

Fig. 8-21 shows a power amplifier circuit. A total of 16 power MOS FETs are used, four each in parallel.

In the SEPP system, since the source electrodes of power supply side MOS FETs Q_1 and Q_1' are connected to the output transformer, an AC coupling system with capacitors and resistors cannot be used. A transformer coupling as shown in Fig. 8-21 is required.

The primary and secondary winding ratio of the input transformer is 1 : 1 (5 turns each) and bifilar winding is used. An E type core is used, but output characteristics vary considerably with the kind of core.

A clock pulse of 140 V_{p-p}, which is the maximum rated voltage for this device, is applied to the gate of the PA stage power MOS FET.

Fig. 8-22 shows theoretical waveforms at different points in Fig. 8-21. Since only carrier signals are used in this case, only the unmodulated carrier component is obtained at the output terminal.

When a pulse-width-modulated wave is applied as a clock pulse to the MOS FET gate, a two-valued PWM wave (1 level: V_{PA} , -1 level: $-V_{PA}$) that has undergone pulse-width modulation with audio frequency is obtained at the output transformer secondary. This PWM wave is filtered in the series resonance circuit consisting of a choke coil and capacitor, and the basic component is derived. Since the crest value of waveform of this basic component varies with pulse width, only the amplitude modulated wave is derived at the output terminal.

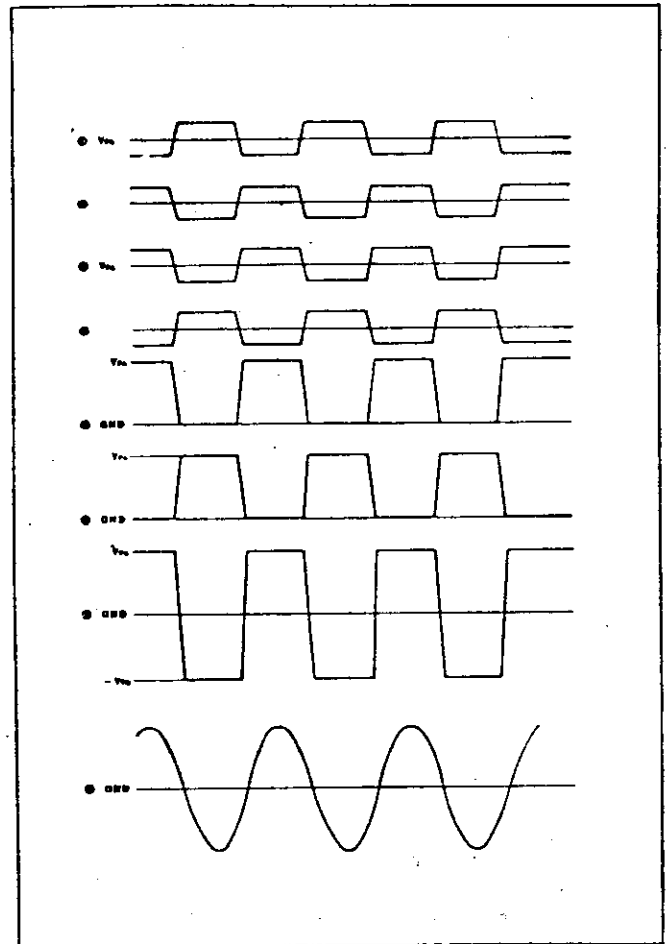


Fig.8-22 Theoretical Waveforms (Unmodulated)

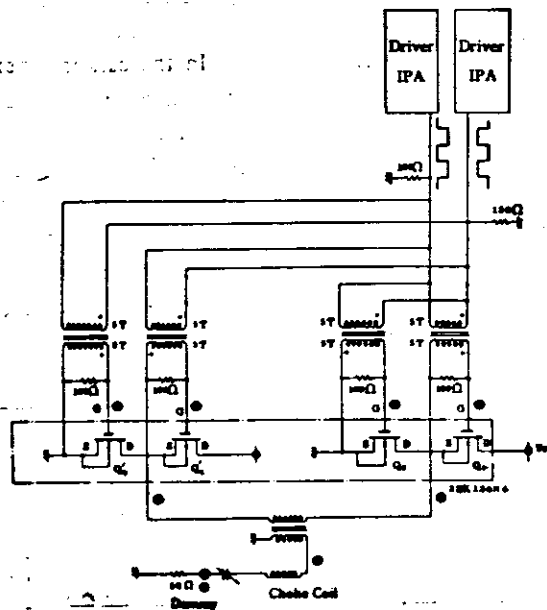


Fig.8-21 PA Circuit in SEPP System

• Output variation by transformer winding ratio

Figs. 8-23 through 8-25 show the dependence of output power and power amplifier efficiency on PA supply voltage at different winding ratios. Fig. 8-26 plots the relationship between PA efficiency and output power with winding ratio as the variable.

While no reference will be made here to transformer types (e.g., core shape, bobbin shape), it has been verified experimentally that use of an E type core and a flat bobbin is effective in achieving high efficiency.

The characteristics shown in Fig. 8-23 through 8-25 are the result of optimum selection based on these tendencies.

From these experiments, it is found that an efficiency of 80 ~ 90% can be expected at PA power supply voltages of 0 ~ 140 V, if the output transformer primary vs. secondary winding ratio is selected at below 1 : 4. Particularly at a winding ratio of 1 : 2, stable operation was obtained at 1.3 kW output power (1 MHz continuous wave) and 87% efficiency.

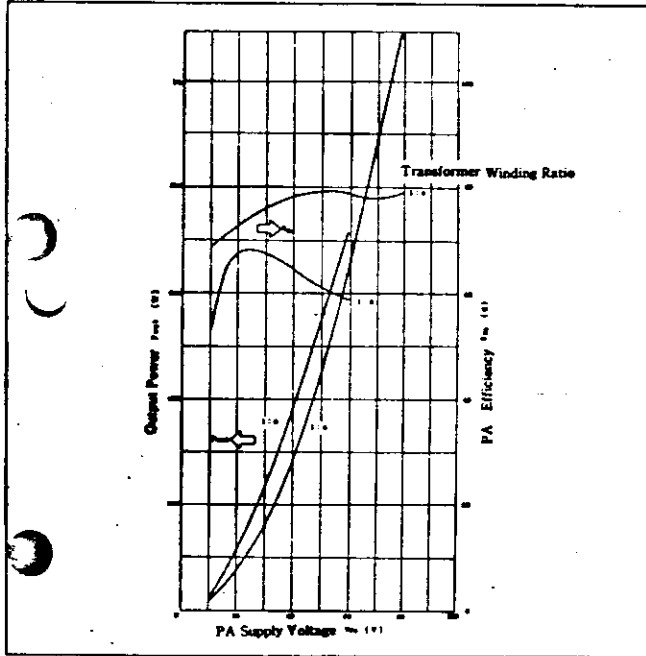


Fig. 8-23 Output Power and PA Efficiency vs. PA Supply Voltage for Various winding Ratio of Transformer

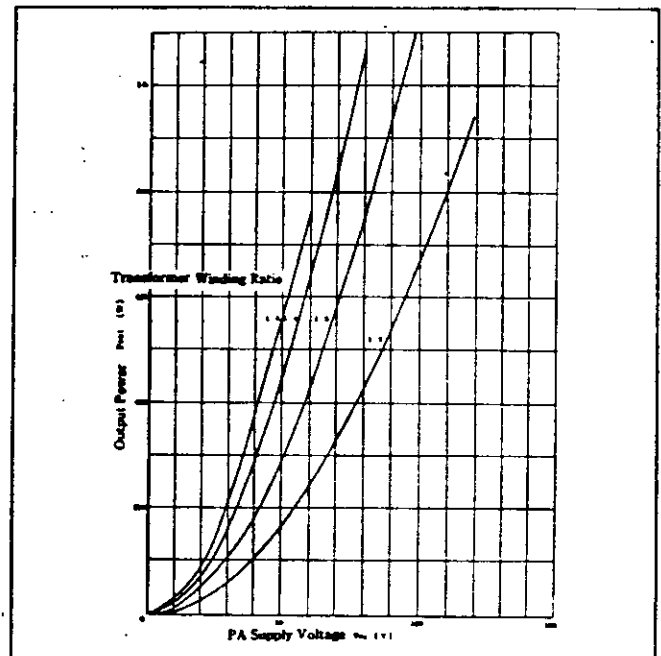


Fig. 8-24 Output Power vs. PA Supply Voltage for Various winding Ratio of Transformer

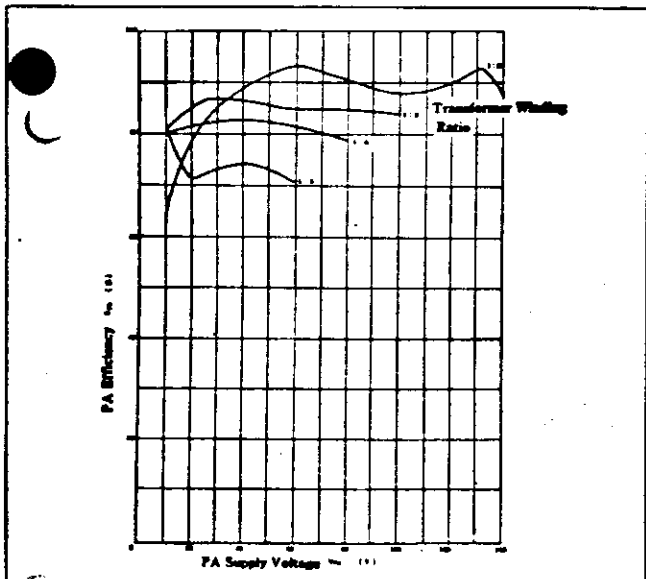


Fig. 8-25 PA Efficiency vs. PA Supply Voltage for Various Winding Ratio of Transformer.

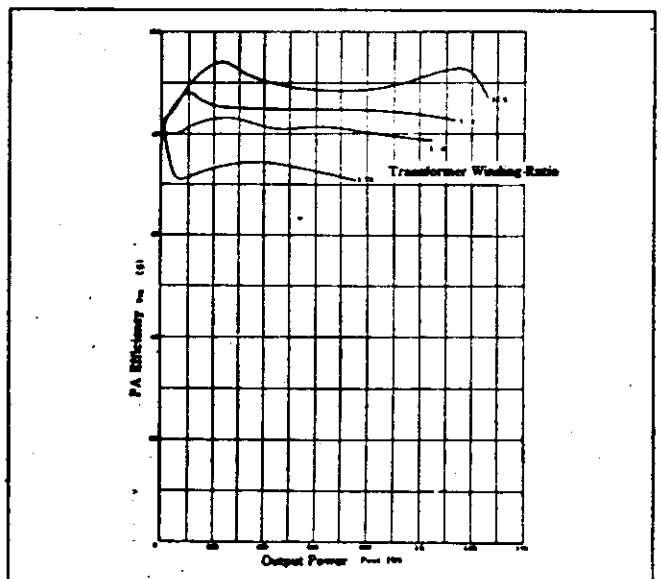


Fig. 8-26 PA Efficiency vs. Output Power for Various Winding Ratio of Transformer

[Reference Data]

Table 8-1 Various Transformer Types

No.	Winding Ratio	Bobbin	Core
F1	Primary : Secondary = 1:2 (Primary : 8 Turns, Parallel in 5) Secondary : 16 Turns, Parallel in 2) Material : Enamel wire ϕ 2mm	Material: Teflon Refer to Fig. 8-27	Insert H6ER-type Ferrite
F2	Primary : Secondary = 1:4 (Primary : 3 Turns, Parallel in 4) Secondary : 12 Turns, Parallel in 2) Material : Enamel wire ϕ 2 mm	—	E-Core Refer to Fig. 8-28(a)
F3	Primary : Secondary = 1:6 (Primary : 2 Turns, Parallel in 4) Secondary : 12 Turns, Parallel in 2) Material : Enamel wire ϕ 2 mm	—	E-Core Refer to Fig. 8-28(a)
F4	Primary : Secondary = 1:2 (Primary : 2 Turns, Parallel in 4) Secondary : 4 Turns, Parallel in 2) Material : Enamel wire ϕ 2 mm	—	E-Core Refer to Fig. 8-28(b)
F5	Primary : Secondary = 1:3 (Primary : 2 Turns, Parallel in 4) Secondary : 6 Turns, Parallel in 1) Material : Enamel wire ϕ 2 mm	—	E-Core Refer to Fig. 8-28(b)

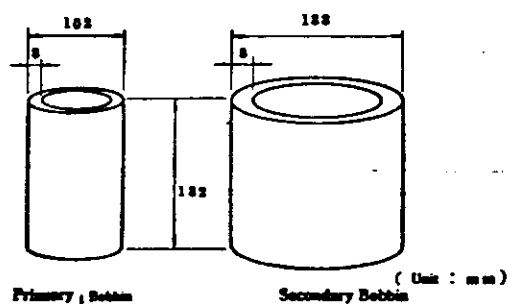


Fig.8-27 Bobbin Shape

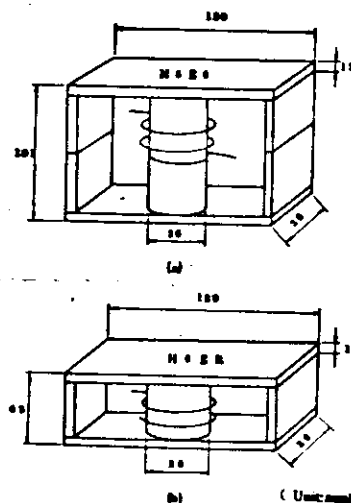


Fig.8-28 E-Core Shape

8.5 High Power Switching Regulators Using Direct Rectification System

Design of a 500 W class switching regulator using power MOS FETs will be introduced. Described below are the features of power MOS FETs as switching devices, followed by calculation of ideal characteristics, design procedure, and measured values.

(1) Advantage of power MOS FETs

Power MOS FETs are capable of high-speed switching, so that the driving circuit is simplified even for frequencies as high as several hundred kHz. Also, when a variable duty ratio control system is used, carrier storage time of the power MOS FET can be neglected, and a wide control range is ensured.

Therefore, output well follows input ripples, and a small filter capacity suffices. This contributes much to improving regulator performance.

Next, switching frequency can be raised to the limit, which is dependent on the performance of the high-speed rectifier diode. Therefore, efficiency can be augmented, equipment can be made compact, and safety improved compared with transistor converters.

(2) Calculation of ideal characteristics

Fig. 8-29 shows a theoretical circuit for a switching regulator. When it is assumed that capacity C is sufficiently large, output E_O is constant, and both switch S and coil L have no loss, then, from the current waveform of Fig. 9-30, the following equilibrium equation holds:

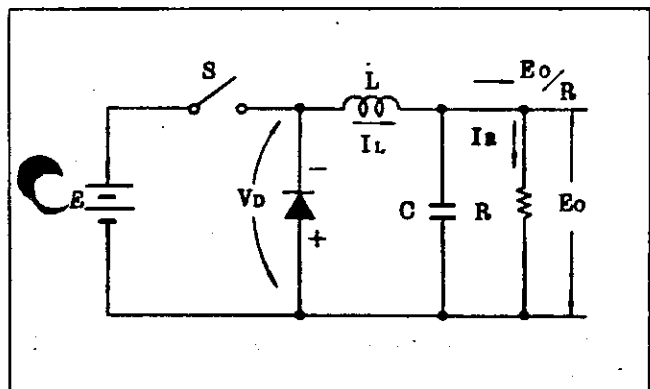


Fig.8-29 Theoretical Circuit for a switching Regulator

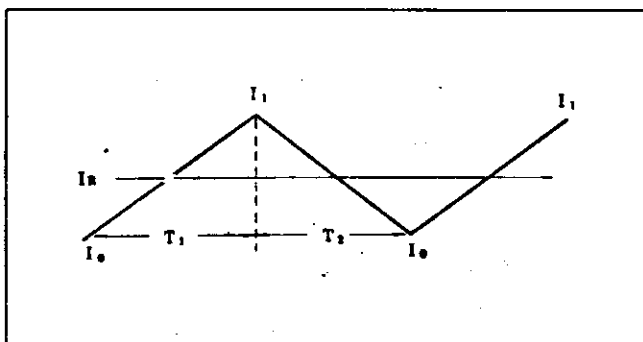


Fig.8-30 Output (Load) Current Waveform

At switch on:

$$L \frac{dI_L}{dt} = E - E_O \quad (1)$$

$$\therefore I_L = \frac{E - E_O}{L} \cdot t + I_0 \quad (2)$$

$$I_1 = \frac{E - E_O}{L} \cdot T_1 + I_0 \quad (3)$$

At switch off:

$$L \cdot \frac{dI_L}{dt} = -(E_O + V_D) \quad (4)$$

$$\therefore I_L = -\frac{E_O + V_D}{L} \cdot t + I_1 \quad (5)$$

$$I_0 = I_1 - \frac{E_O + V_D}{L} \cdot T_2 \quad (6)$$

$$\text{Thus, } (E - E_O)T_1 = (E_O + V_D)T_2$$

$$\text{Therefore, } E_O = E \cdot \frac{T_1}{T} - V_D \cdot \frac{T_2}{T} \text{ where } T = T_1 + T_2 \quad (7)$$

Mean load current I_R will be:

$$I_R = \frac{I_1 + I_0}{2} \quad (8)$$

Next, if I_0, I_1 is denoted by I_R , then

$$I_1 = I_R + \frac{E - E_O}{2 \cdot L} \cdot T_1 \quad (9)$$

$$I_0 = I_R - \frac{E - E_O}{2 \cdot L} \cdot T_1 \quad (10)$$

Since minimum load current I_0 is larger than 0, from Equation (10), the minimum value for coil L will be:

$$L_{\min} = \frac{E - E_O}{2I_R} \cdot T_1 \quad (11)$$

If the variation value of load current is put as $\Delta I = I_1 - I_0$, then, from Equations (9) and (10), we get

$$\Delta I = \frac{E - E_O}{L} \cdot T_1 \quad (12)$$

If variation ratio is put as $\alpha = \Delta I / I_R$, then the required L value is determined as

$$L = \frac{E - E_O}{\alpha I_R} \cdot T_1 \quad (13)$$

To seek conduction angle T_1/T , from Equation (7), we get

$$E_O = E \cdot \frac{T_1}{T} - V_D \left(1 - \frac{T_1}{T}\right)$$

Therefore,

$$\frac{T_1}{T} = \frac{E_O + V_D}{E + V_D} \quad (14)$$

Next, let us seek the values of power and efficiency.

$$\begin{aligned} \text{Input power } W_i &= \frac{E}{T} \int_0^{T_1} \left(\frac{E - E_O}{L} \cdot t + I_O \right) dt \\ &= \frac{E}{T} \left(\frac{E - E_O}{2L} \cdot T_1^2 + I_O \cdot T_1 \right) \end{aligned}$$

Substituting Equations (9) and (10) into this, we get

$$\begin{aligned} W_i &= \frac{T_1}{T} \cdot E \left(\frac{I_1 - I_O}{2} + I_O \right) \\ &= \frac{T_1}{T} \cdot E \cdot I_R = E \cdot \frac{E_O + V_D}{E + V_D} \cdot I_R \quad (15) \end{aligned}$$

Output power

$$W_O = E_O \cdot I_R \quad (16)$$

Output efficiency

$$\eta = \frac{W_O}{W_i} = \frac{E_O}{E} \cdot \frac{E + V_D}{E_O + V_D} \quad (17)$$

Power loss W_D of the rectifier diode is given as:

$$\begin{aligned} W_D &= V_D \cdot \frac{1}{T} \int_0^{T_2} \left(I_1 - \frac{E_O + V_D}{L} t \right) dt \\ &= V_D \cdot \frac{1}{T} \left(I_1 \cdot T_2 - \frac{E_O + V_D}{2L} \cdot T_2^2 \right) \\ &= \frac{V_D}{T} \left(I_1 \cdot T_2 - \frac{I_1 - I_O}{2} \cdot T_2 \right) = V_D \cdot I_R \cdot \frac{T_2}{T} \\ &= V_D \cdot \frac{E - E_O}{E + V_D} \cdot I_R \quad (18) \end{aligned}$$

$$\text{Thus, } W_i = W_L + W_D = (E_O + V_D) \cdot \frac{E - E_O}{E + V_D} \cdot I_R$$

$$= E \cdot \frac{E_O + V_D}{E + V_D} \cdot I_R \quad (19)$$

• Typical values

If it is assumed that $E = 100 \text{ V}$, $E_O = 50 \text{ V}$, $W_L = 200 \text{ W}$, $V_D = 1 \text{ V}$, $I_R = 4 \text{ A}$, $f = 80 \text{ kHz}$ ($T = 12.5 \mu\text{s}$), then $T_1 = 3 \mu\text{s}$.

$$\text{When } \alpha = 0.5, \text{ then } L = \frac{E - E_O}{0.5 I_R} \cdot T_1 = 157 \mu\text{H},$$

$$\eta = 0.99 \text{ (99\% efficiency)}$$

Efficiency increases as input, output voltage ratio E_O/E approaches 1.0. In designing an actual switching regulator, losses and optimum values must be calculated individually for the main power supply, switching circuit, control circuit, and filter circuit.

(3) Typical design

• Basic design philosophy

- Maximum output 500 W
- Variable voltage range 10 ~ 100 V
- Input power 500 W
- Input voltage 140 V
- Type of circuit Input part is a 100 V AC direct bridge rectification system; power MOS FETs are driven by capacitance-coupling and controlled by variable duty type control.

- Switching frequency 40 kHz (25 μs)

Rectifier diodes currently available have a reverse breakdown voltage of 300 V, a maximum current of 6 A, a reverse recovery time of 0.2 μs , and a forward voltage of 0.8 V or so. If these performance figures are improved, switching can be performed at higher frequencies.

- The sensing output voltage feedback loop is isolated by a photo coupler.
- Output transformer 20 : 18 in turns; EIH-90. winding ratio and core
- Cautions in fabrication
- Since the output transformer winding is subject to sharp current spikes, it is required to have a large capacity. Vinyl wire is recommended.
- Providing a center tap on the output transformer's secondary winding and using full-wave rectification are effective in reducing rectifier diode loss. (In the example described below, the bridge rectification system is used for both primary and secondary windings.
- A large capacity choke coil should be used in order to maintain a constant current over a wide range.

• Circuit operation

The basic circuit configuration of this regulator is shown in Fig. 8-31.

In the sensing block, the voltage at the output terminal is divided and compared with the reference voltage generated by a Zener diode, and the error voltage is output.

Here, a single operational amplifier IC, HA17741, is used in the error amplification circuit and the overcurrent limitation circuit. The circuit configuration is a standardized one.

In the control block, a variable duty circuit is used to reduce noise.

The power MOS FET has a switching speed as fast as 20 ~ 30 ns and is liable to generate noise. Also, its high input impedance can induce external noise, which in turn can

cause misoperation.

In the variable duty circuit, therefore, rectangular waves in which the direct current component is superposed on the AC signal are integrated and the voltage comparator is operated at the cross-zero point.

As a result, the loop has a low response speed but is not affected by noise.

The drive block uses the CMOS inverter IC HA14011B which drives the power MOS FETs and a complementarily connected 200 mW class transistor. This block illustrates

the characteristic ease of use of power MOS FETs. The driver need only have an input power of 10 V and a charge/discharge capacity of 1,000 pF. The drive circuit is vastly simplified. If it is assumed that the power MOS FET rise time t_r is 30 ns, then, one only has to consider the 300 mA transient current and the approximately 0 mA steady state current (there is a slight leak current).

The circuitry of the blocks described above is presented in Figs. 8-32 through 8-34.

Fig. 8-35 shows a timing chart for the control block.

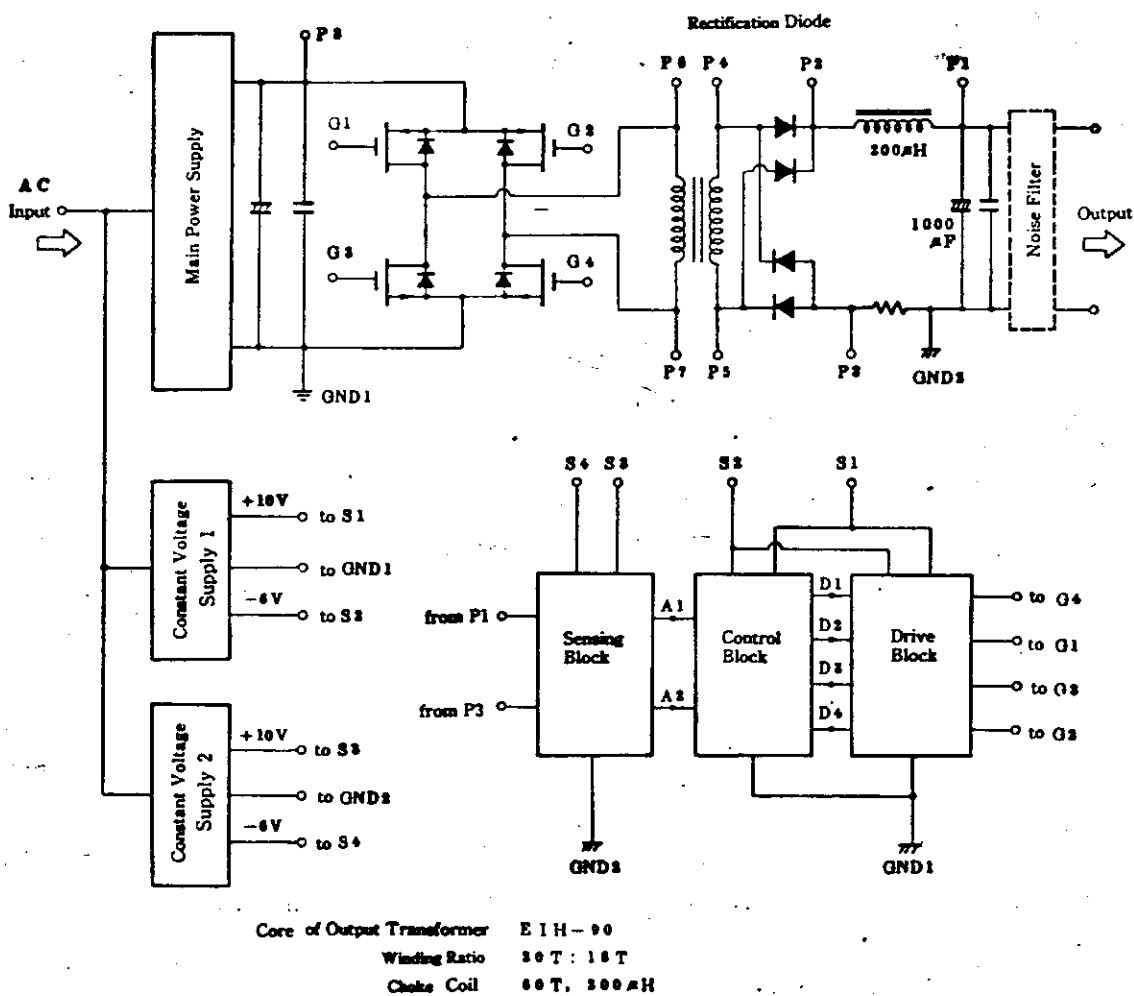


Fig.8-31 Block Diagram of High Power Switching Regulator

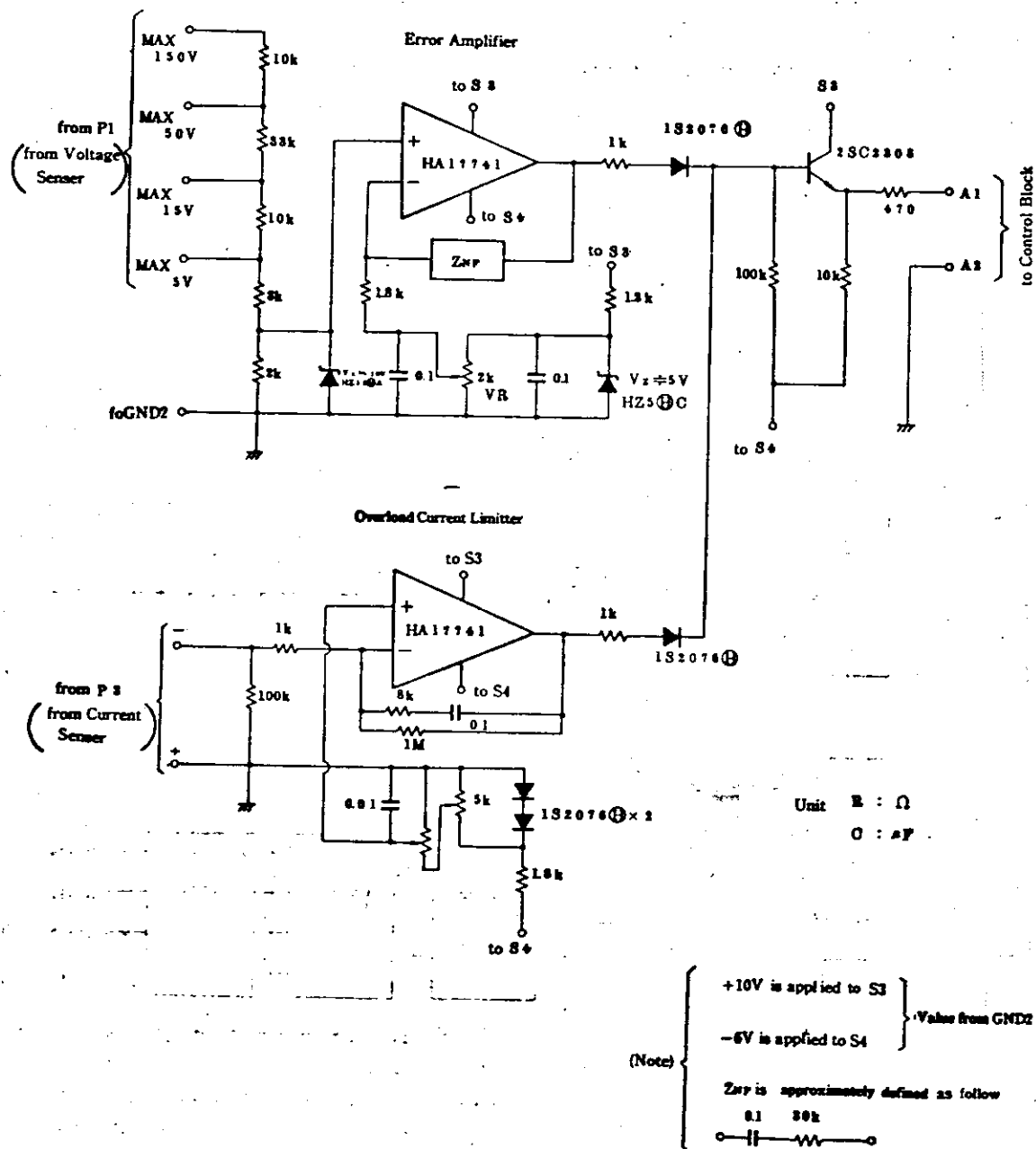
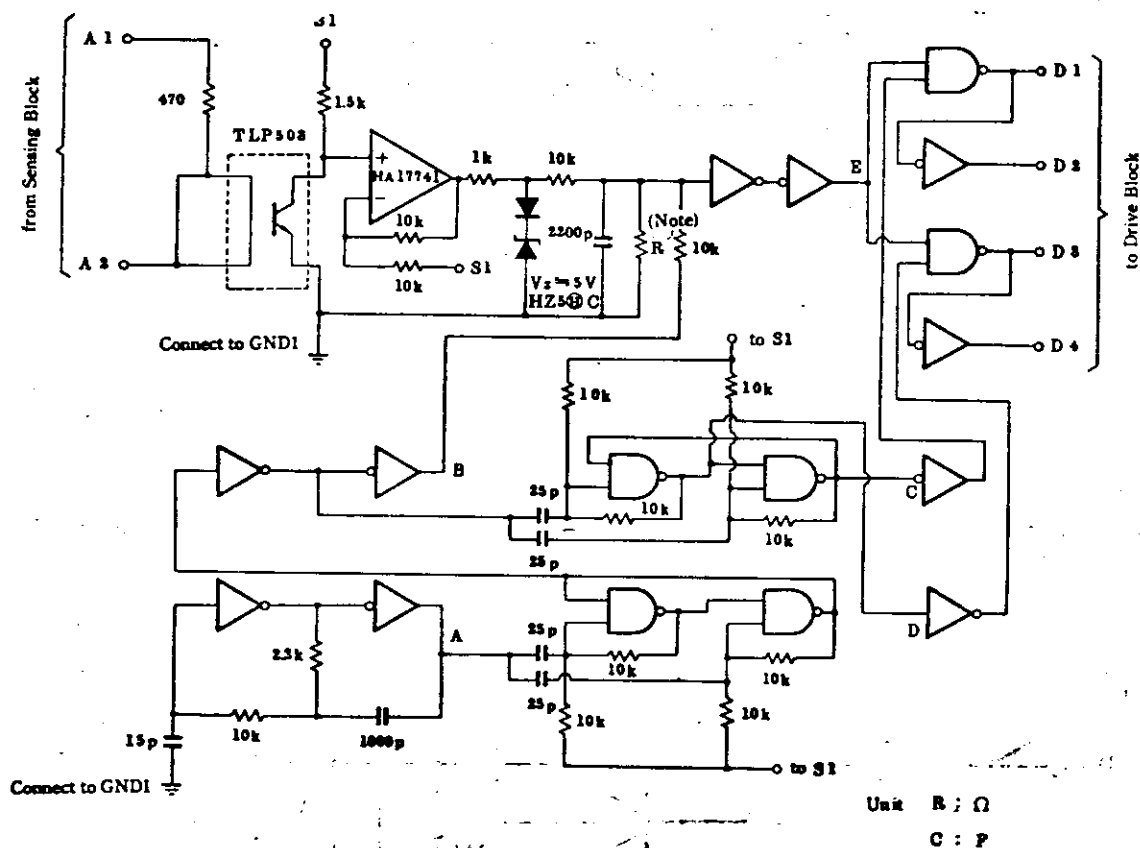


Fig.8-32 Sensing Block



$\left. \begin{array}{l} +15V \text{ is applied to } S1 \\ -10V \text{ is applied to } S2 \end{array} \right\} \text{Values from GND1}$

• HD14011B is used for all gates.

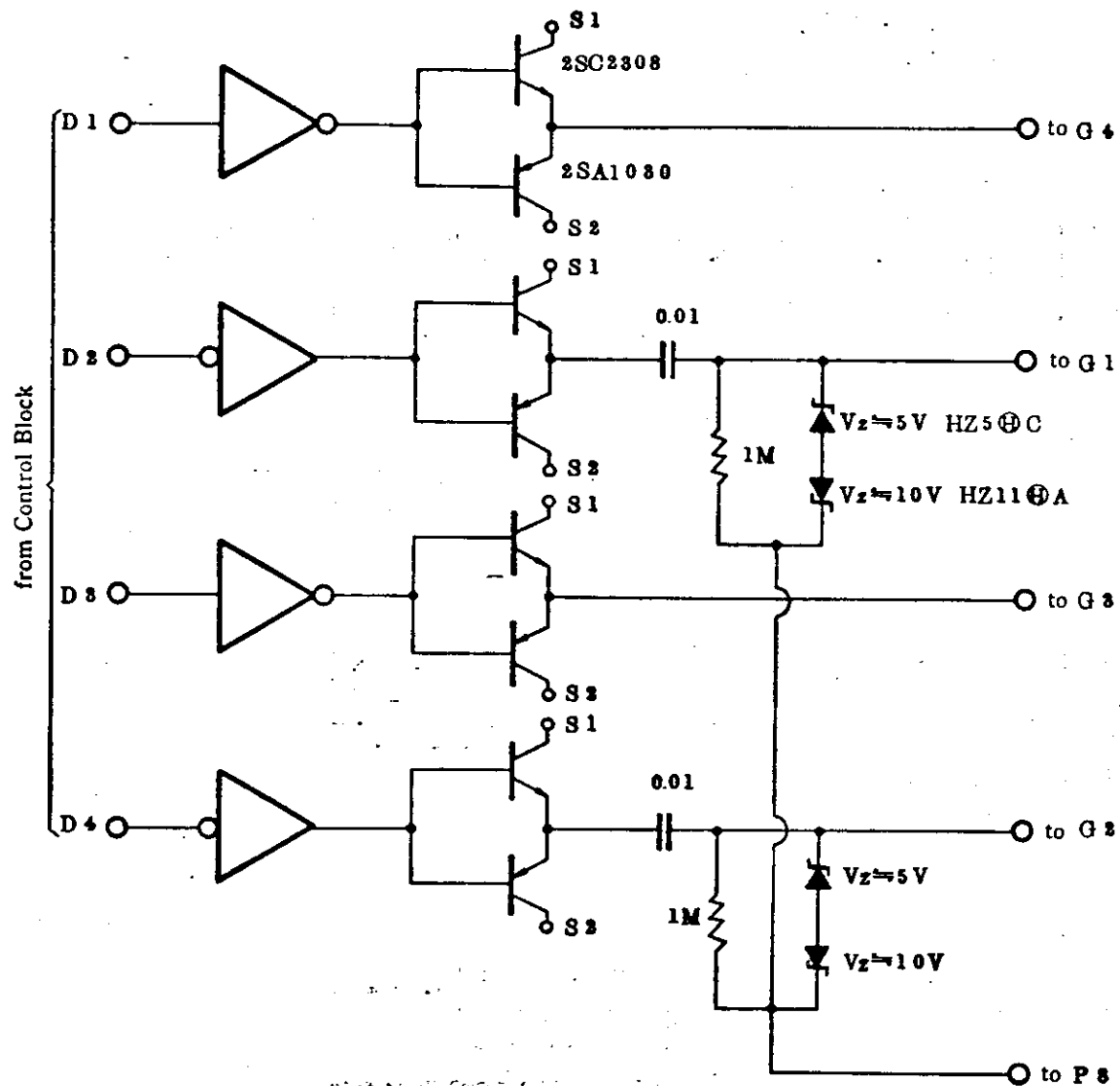
For the inverter, it is necessary that one gate is pulled-up to S1. (Do not use 2 gate in parallel)

• The supply voltage S1 and S2 should be given to HA17741 and HD14011B

• R must be adjusted to determine the dead time.

The value will be approximately 10 k Ω .

Fig.8-33 Control Block



Unit R : Ω
C : pF

(Note)

- For the inverter, HD14011B is used with one gate Pulled-up to S1.
- S1 is +10V, and S2 is -6V.
- S1 and S2 should be given to V_{DD} and V_{SS} of HD14011B respectively.
- The transistors are 4 pairs of 2SC2308 & 2SA1030.

Fig.8-34 Drive Block

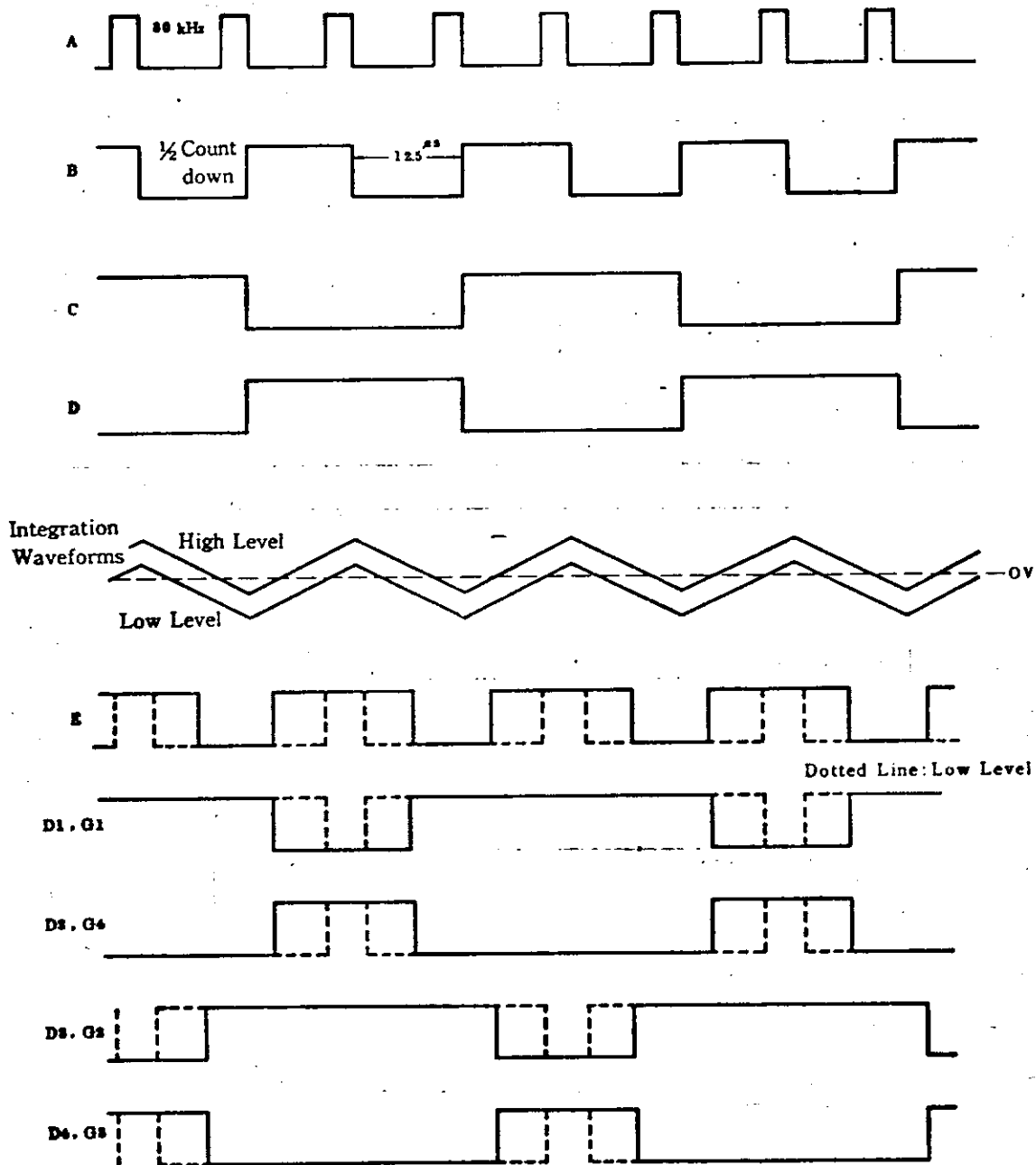


Fig. 8-35 Theoretical Waveforms in Control Block

8. Designing Application Circuits

• Nominal characteristics of experimental circuit

Figs. 8-36 and 8-37 show voltage waveforms, respectively, for the output transformer secondary and differential voltage between choke coil terminals. It will be seen that the conduction angle follows the specified output. Under the operating conditions of 80 V and 3 A, the duty factor is

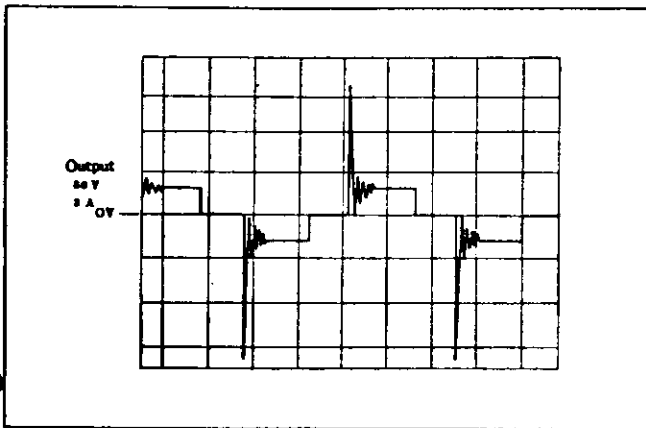


Fig. 8-36 Voltage Waveforms for the Transformer Secondary

about 70%. Other characteristics illustrated are the following:

Fig. 8-38 Regulation characteristics

Fig. 8-39 Efficiency vs. output current characteristics (V_O constant)

Fig. 8-40 Efficiency vs. output voltage characteristics (I_O constant)

Fig. 8-41 Efficiency vs. output current characteristics (P_O constant)

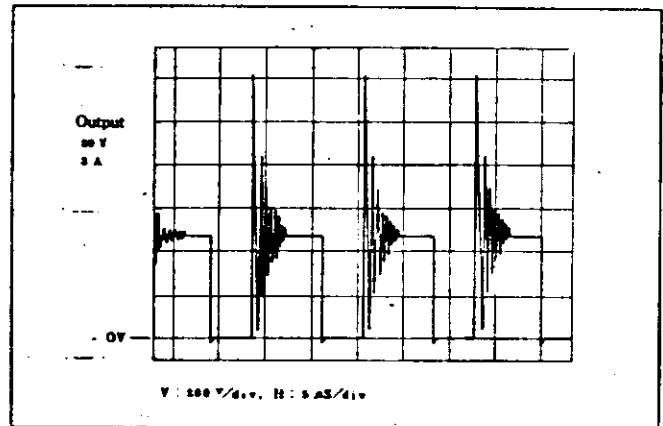


Fig. 8-37 Voltage Waveforms for the Differential Voltage between Choke Coil Terminals

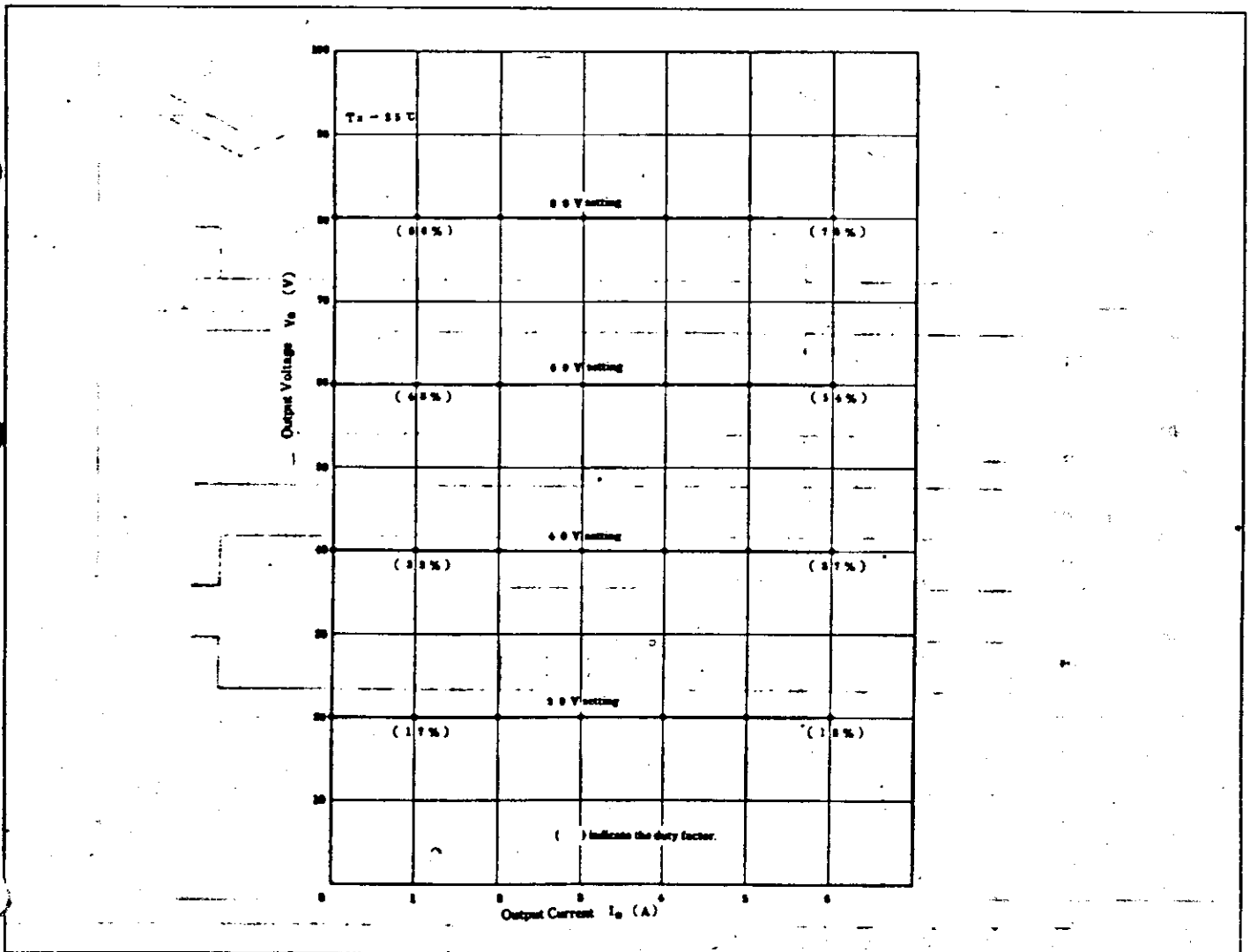


Fig. 8-38 Regulation Characteristics

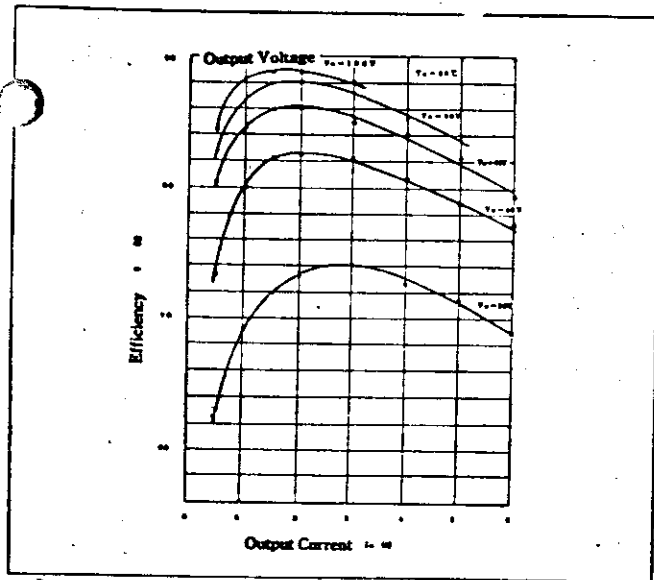


Fig. 8-39 Efficiency vs. Output Current Characteristics (V_o constant)

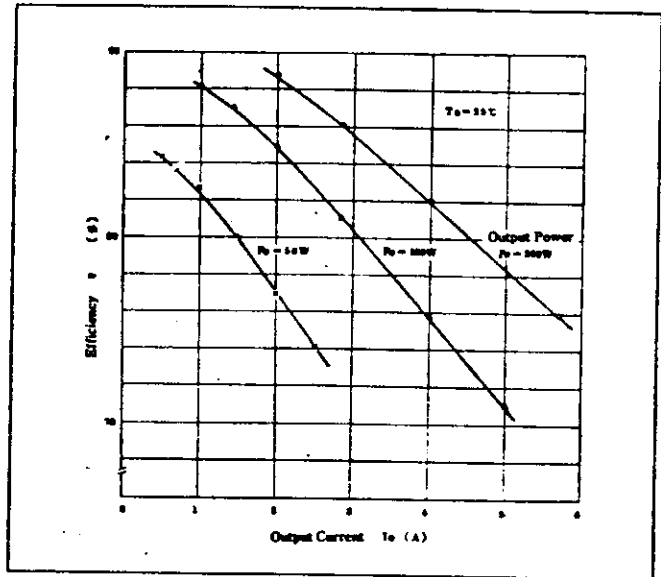


Fig. 8-41 Efficiency vs. Output Voltage Characteristics (P_o constant)

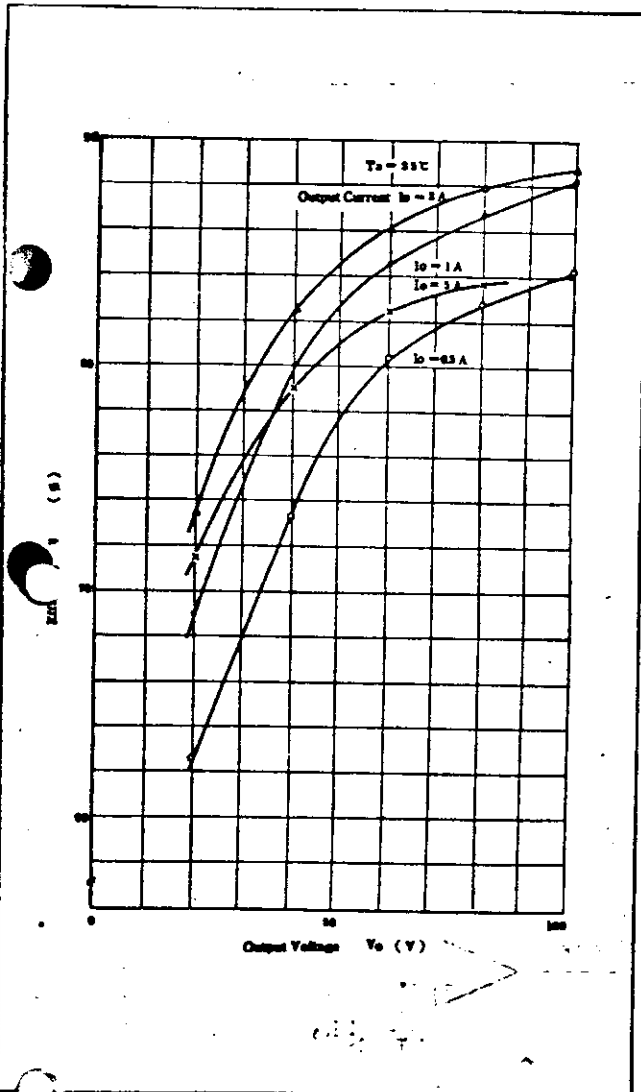


Fig. 8-40 Efficiency vs. Output Voltage Characteristics (I_o constant)

8.6 Low-Noise DC-DC Converters

The converter introduced here is based on a design philosophy different from that of the high-power, high-efficiency switching regulator described in the preceding chapter.

Spike noise has been reduced to the limit in this converter, so that it can be used in the PCM decoder part of electronic switching systems which are sensitive to noise at the small signal level.

The circuitry and test results are described below.

(1) Circuit configuration and operation

A block diagram is presented in Fig. 8-42. It is a single-transistor converter using a power MOS FET as the main switch. Low noise is achieved by:

- effectively utilizing the electrode structure of power MOS FETs (source electrode is connected to header), and

- loosely coupling the output transformer.

For driving and controlling the power MOS FET, a CMOS gate IC is employed.

A 12 V, 5 mA subsidiary power supply is provided by dividing the voltage at the AC input.

The control loops are isolated by means of a photo coupler of 4 MHz bandwidth.

Radiation can be coped with by a shield plate; there is no need for a special noise filter. (When the converter was mounted in a PCM decoder, crosstalk to the adjacent channel was below -90 dBm/20 kHz.)

Since carrier storage effect can be neglected in driving a power MOS FET, a mirror integration circuit is formed with C_2 and the transformer primary, as shown in Fig. 8-42. As a result, the switching waveform draws a gentle slope and the spike component is completely removed.

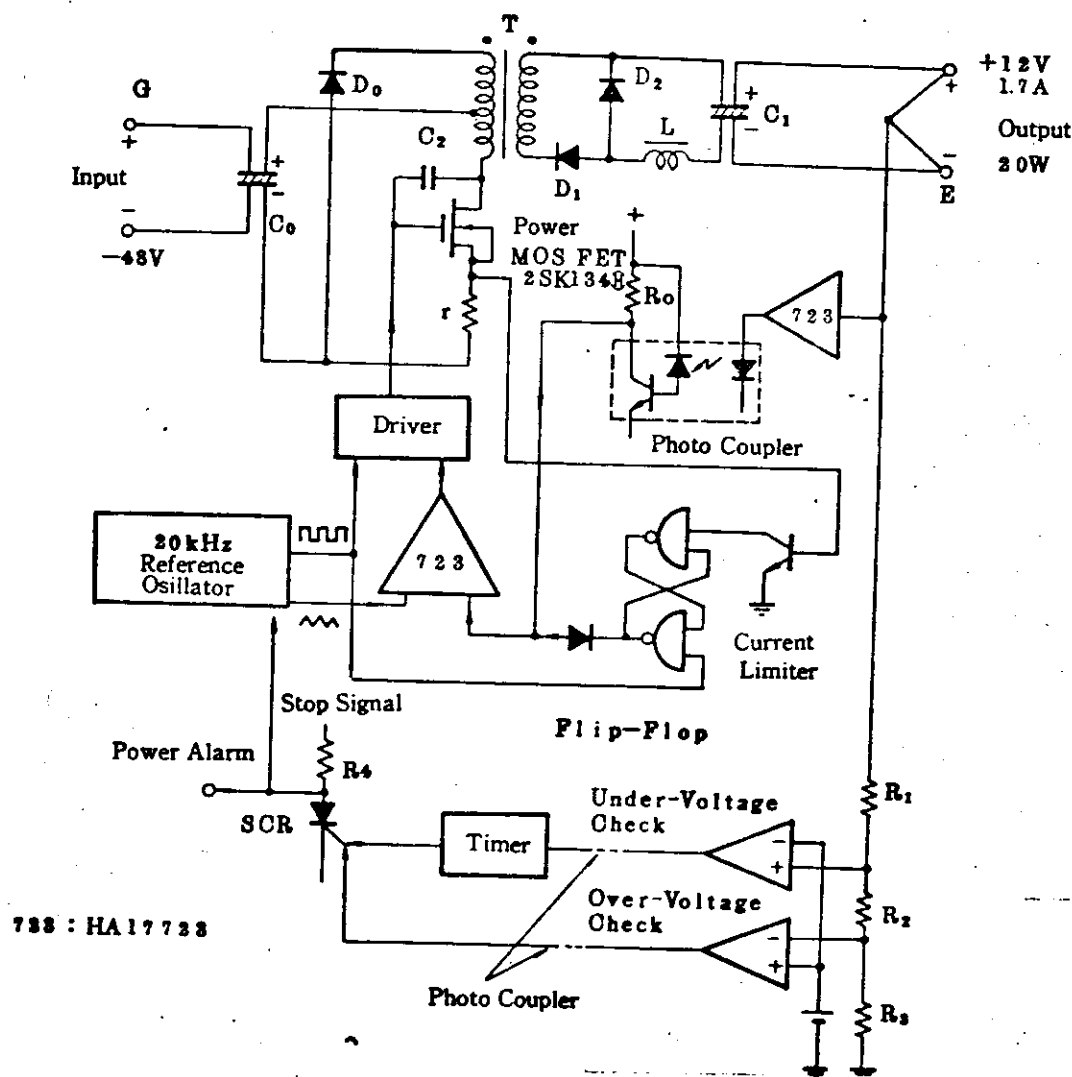


Fig. 8-42 Block Diagram of DC-DC Converter

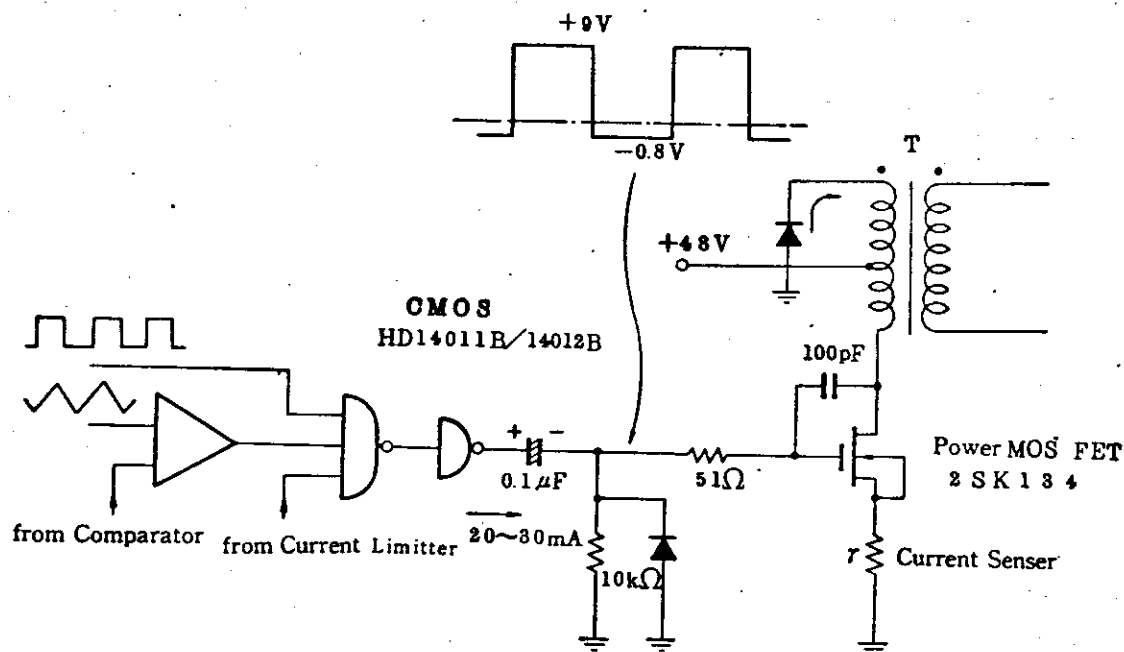


Fig.8-43 Drive Circuit for DC-DC Converter

Results of experiment

Major performance figures are shown in Table 8-2. By taking advantage of the performance, circuits that produce the desired output voltage and current can be designed.

Table 8-2 Major Performance Figures

Item	Condition	Performance
Input Voltage	-	-48±5V
Output Voltage, Current	Full load	+12V, 1.7A
Spike Voltage	Full load	4mVp-p
Regulation for Input Voltage Changes	-48V → -53V	+2mV
Regulation for Load Changes	Non load → Full load	-17mV
Efficiency	Full Load Full Circuit	71%

Figs. 8-44 and 8-45 show operation waveforms of the power MOS FET, and Fig. 8-46 the output terminal ripple and spike noise waveforms.

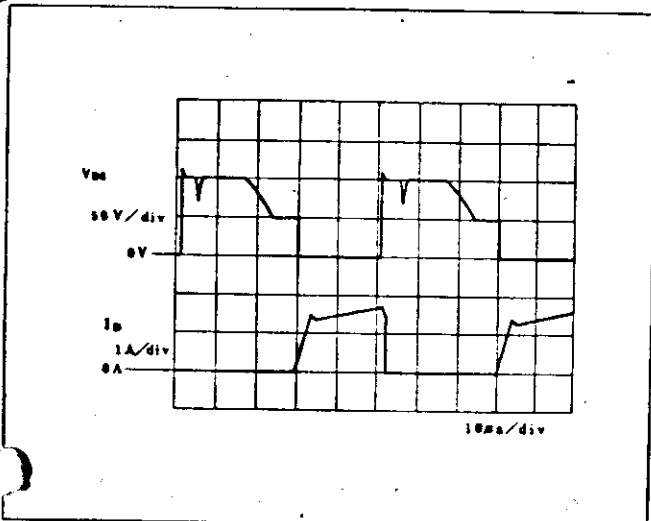


Fig. 8-44 Operation Waveforms of Power MOS FET

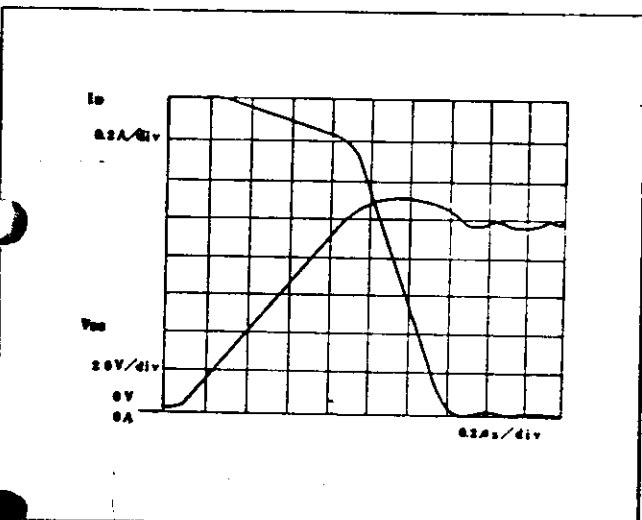


Fig. 8-45 Operation Waveforms of Power MOS FET

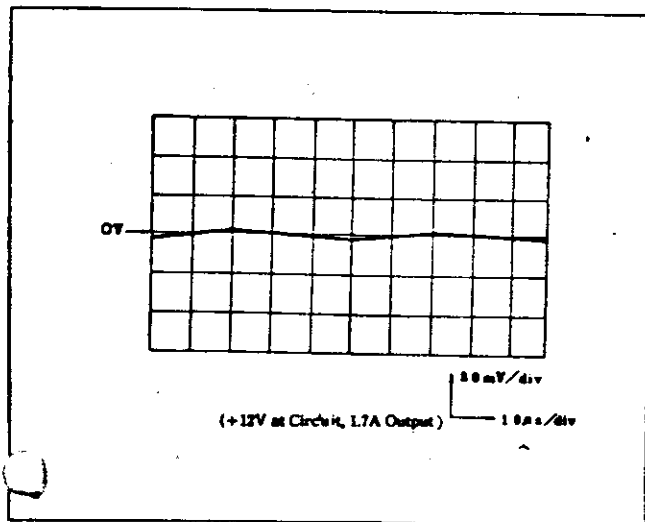


Fig. 8-46 Ripple and Spike Noise Waveforms